博士論文番号：1481208
(Doctoral student number)

# Induction of the unfolded protein response pathway upon diauxic shift of yeast cells and its involvement in mitochondria enlargement

（出芽酵母の Diauxic shift 時における unfolded protein response 経路の活性化と、それに伴うミトコンドリア伸展）

Tran Minh Duc

Nara Institute of Science and Technology
Graduate School of Biological Sciences
Applied Stress Microbiology Laboratory

(Supervisor’s name: Assoc. Prof. Yukio Kimata)

2018/07/30

Graduate School of Biological Sciences　Doctoral Thesis Abstract

| | | | |
|---|---|---|---|
| Lab name<br>(Supervisor) | Applied Stress Microbiology<br>(Assoc. Prof. Yukio Kimata) | | |
| Name<br>(surname) (given name) | Tran Minh Duc | Date | 2018/07/30 |
| Title | Induction of the unfolded protein response pathway upon diauxic shift of yeast cells and its involvement in mitochondria enlargement | | |


## Abstract

The endoplasmic reticulum (ER) is a membrane-bound cellular compartment in which secretory and transmembrane proteins are folded. Accumulation of unfolded proteins in the ER, which results from or in dysfunction of the ER, is called ER stress, and triggers the unfolded protein response (UPR) commonly in eukaryotic cells. Ire1, an ER-located type-I transmembrane endoribonuclease conserved through eukaryotic species, serves as an ER-stress sensor that triggers the UPR. In ER-stressed *Saccharomyces cerevisiae* (hereafter simply called yeast) cells, the *HAC1* mRNA is spliced by Ire1 and then translated into a transcription-factor protein, which works for the UPR transcriptional induction. While Ire1 is activated through directly capturing unfolded proteins accumulated in the ER, it is also known that certain stressing stimuli, such as membrane-lipid aberrancy, activate Ire1 and trigger the UPR independently of ER accumulation of unfolded proteins. In my present study, I thus addressed a new scene which evokes the UPR without damaging ER protein-folding status in yeast cells.

When cultured in rich medium containing fermentable sugar, such as glucose, yeast cells utilize it without respiration, namely fermentation, resulting in their fast growth. On the other hand, upon exhaustion of the sugar, cells predominantly get energy through aerobic respiration using the fermentation products, and grow rather slowly. This change from fermentation to respiration is named as diauxic shift, which is accompanied with a substantial alteration of cellular gene-expression profile and with massive expansion of mitochondria. In this thesis, I describe induction of the UPR in response to diauxic shift in yeast cells.

Here I checked activity of Ire1 and the UPR evocation in yeast cells by monitoring the *HAC1*-mRNA splicing, which, according to my observation obtained from this study, was transiently induced upon diauxic shift. Moreover, the UPR was continuingly induced when cells were shifted to non-fermentable glycerol-based medium. However, diauxic shift did not seem to impair protein folding in the ER. In contrast, my data cumulatively suggest that reactive oxygen spices (ROS), which are known to be byproducts of respiration, contribute to the activation of Ire1 in this case. This insight, which argues for a case that oxidative stress leads to the UPR, is contrasting against a canonical concept that reductive stress but not oxidative stress predominantly impairs protein folding in the ER and activates Ire1.

Meanwhile, ROS does not seem to be the sole regulator for Ire1's transient activation upon diauxic shift. According to my observations obtained in the present study, the luminal domain of Ire1 is also involved in upregulation of Ire1 upon diauxic shift together with its downregulation on the post-diauxic shift.

Gene knock-out analyses indicated that Ire1 and the *HAC1* gene contribute to cellular growth after diauxic shift. In order to address the molecular basis underlying requirement of the UPR pathway in this case, I have checked gene expression profile in *IRE1*+ cells and in *ire1* knock-out cells by using the RNA reverse-transcription and second-generation DNA-sequencing techniques. As a result, while the Ire1-dependent gene-expression change induced by diauxic shift and that caused by tunicamycin, which inhibits N-glycosylation of ER proteins, was highly similar, genes encoded on the mitochondria genome were totally induced dependently on Ire1 upon diauxic shift but not upon cellular treatment with tunicamycin. My further analysis indicated the Ire1-*HAC1* pathway of the UPR contributes to mitochondrial expansion alongside diauxic shift. Consistently with this insight, aerobic respiration was poorly induced upon diauxic shift in *ire1* knock-out cells.

Taken together, my study have disclosed a new regulatory mechanism and role of the yeast UPR pathway. I thus propose a novel positive regulatory loop, in which ROS activates Ire1, which contributes to mitochondrial expansion, which then stimulates respiration and ROS production.

# CONTENTS

## CONTENTS (Cont.)

## LIST OF ABBREVIATIONS

BiP: Binding Immunoglobulin Protein

bZIP: Basic Leucine Zipper domain

DTT: Dithiothreitol

ER: Endoplasmic Reticulum

ERAD: ER-Associated Protein Degradation

Hac1: bZIP transcription factor

Hsp70: 70 kDa heat shock protein

Ire1: Inositol-requiring enzyme 1

NGS: Next Generation Sequencing

RT-PCR: Reverse transcription polymerase chain reaction

RT-qPCR: Reverse transcription quantitative polymerase chain reaction

ROS: Reactive Oxygen Species

SD: Synthetic Dextrose

TM: Tunicamycin

UPR: Unfolded Protein Response

UTR: Untranslated Region

UPRE: Unfolded Protein Response Element

YPD: Yeast Extract-Peptone-Dextrose

# LIST OF FIGURES

# LIST OF TABLES

# CHAPTER I
# INTRODUCTION

## 1.1. The UPR and Ire1 in *Saccharomyces cerevisiae* cells

Eukaryotic cells commonly carry the endoplasmic reticulum (ER), which is a membrane-bound sac taking a tubular or flat shape and being expanded throughout cells. When budding yeast *S. cerevisiae* cells producing an exogenous ER-located fluorescent protein are observed under fluorescence microscope, its distribution exhibits a double-ring-like pattern (Fig. 1). The outer ring, which is adjacently located to the plasma membrane, is named the cortical ER. Meanwhile, the inner ring is identical to the nuclear envelop and also functions as the ER.

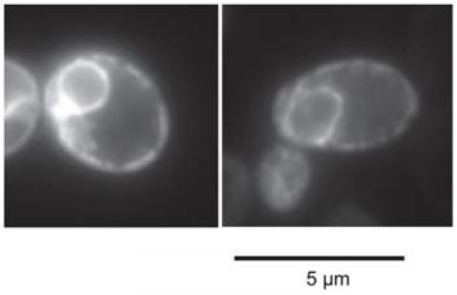


**Fig. 1 The ER in yeast cells.**
Yeast cell producing an ER-located version of GFP were observed under a fluorescent microscope.

The ribosomes are attached on the ER membrane to form the rough ER. The ER, which bears some molecular chaperones and protein folding enzymes, works as the location in which secretory and transmembrane proteins are folded to take high-order structures. Whereas "binding immunoglobulin protein" (BiP) was initially isolated from mammalian antibody-making cells as a protein associating with premature immunoglobulin heavy chain, it is conserved throughout eukaryotic species including fungi and yeast (Normington et al., 1989; Rose et al., 1989). BiP is now known as an ER-located molecular chaperone, which functions both for ER translocation and for folding of client proteins. Proteins correctly folded in the ER is then packed into the COPII transport vesicles and carried to other cellular compartments including cell surface via the Golgi apparatus. The ER also acts as the site where membrane-lipid components are biosynthesized.

In many cases, dysfunction of the ER, which is collectively called ER stress, results from or in misfolding and aggregation of ER client proteins. For instance, many of ER client proteins are N-glycosylated during their translocation into the ER, and thus its disturbance is known to induce potent ER stress. Disulfide-bond formation between two cysteine residues is another important protein-modification event performed in the ER, and contributes to oxidative protein folding. Therefore, impaired disulfide-bond formation of proteins causes serious ER stress.

As initially observed in a mammalian study performed by Kozutsumi et al. (1998), ER stress transcriptionally induces BiP. This phenomenon is called the ER stress response or the

unfolded protein response (UPR), the molecular mechanism of which has then been predominantly uncovered through pioneer studies using the easy-to-use unicellular eukaryotic model organism, namely *S. cerevisiae*. Mori et al. (1992) and Kohno et al. (1993) reported an UPR-responsive promoter element on the *S. cerevisiae* BiP gene. Moreover, Ire1 was identified through genetic screening for *S. cerevisiae* mutants in which the UPR is impaired (Mori et al., 1993; Cox et al., 1993).

Ire1 is conserved through eukaryotic species and is an ER-located type-I transmembrane protein. As shown in Fig.2, the cytosolic domain of Ire1 acts both as a Ser/Thr protein kinase and as an endoribonuclease (Mori et al., 1993; Sidrauski and Walter, 1997). The kinase activity of Ire1 contributes to trans-auto-phosphorylation of self-associated Ire1 molecules, which then triggers the UPR (Shamu and Walter P; 1996). Therefore, kinase-dead mutants of Ire1 can evoke the UPR if they take a structure that mimics the phosphorylated form (Papa et al., 2003; Chawla et al., 2011; Rubio et al., 2011). The kinase domain also functions for capturing ADP, which, as well as the auto-phosphorylation of Ire1, is required for activation of Ire1 (Lee et al., 2008; Korennykh et al., 2009; Rubio et al., 2011). On the other hand, the endoribonuclease activity of Ire1 *per se* is the effector that initiates the downstream events for intracellular signaling in the UPR (Cox and Walter, 1996; Sidrauski and Walter, 1997).

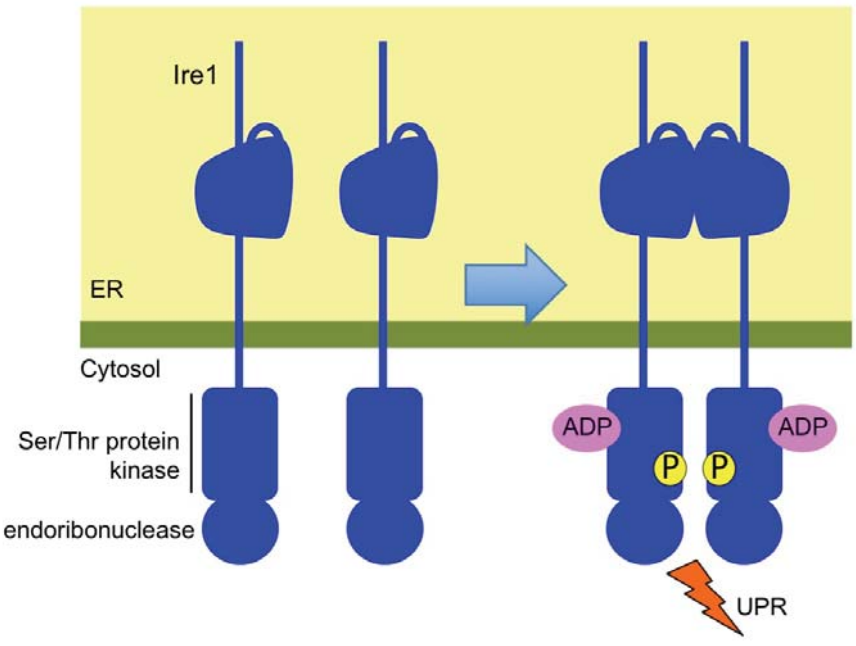


**Fig. 2 Activation of Ire1.**

Ire1 is activated as an endoribonuclease via its self-association, auto-phosphorylation and capturing ADP.

The downstream target of Ire1 is encoded on the *HAC1* gene, which has been identified through multiple experimental approaches including a genetic screening for multicopy suppressors of the *IRE1*-knockout mutation (Cox and Walter, 1996; Mori et al., 1996; Nikawa et al., 1997). As shown in Fig. 3A, Ire1 acts as an endoribonuclease which splices the *HAC1* mRNA (Cox and Walter, 1996; Sidrauski and Walter, 1997). The tRNA ligase Rlg1 participates to this reaction by joining two exons (Fig. 3B; Sidrauski et al., 1996; Sidrauski and Walter, 1997). Therefore, as also demonstrated by Kawahara et al. (1998) and Gonzalez et al. (1999), the Ire1 and Rlg1-dependent splicing of the *HAC1* mRNA in the cytoplasm mechanistically differs from the spliceosome-dependent conventional mRNA splicing that is carried out in the nuclei.

The spliced form of the *HAC1* mRNA (*HAC1*$^{i}$; “i" for induced) is effectively translated into a basic leucine zipper (bZIP)-family transcription factor that is directly bound to the promoter elements of the UPR-target genes and evokes the UPR. On the other hand, translation of the unspliced *HAC1* mRNA (*HAC1*$^{u}$; “u" for uninduced) is tightly suppressed through its intramolecular hybridization between the 5’-untranslated region (UTR) and the intron (Fig. 3B; Rüegsegger et al., 2001). Moreover, the *HAC1*$^{u}$ protein has only weak activity as a transcription factor, and is degraded quickly by the proteasome (Mori et al., 2000; Santo et al., 2016).

In addition to the BiP genes, there exists a wide variety of genes the expression of which is under the control of the Ire1 and *HAC1*-dependent UPR. Casagrande et al. (2000) and Friedlander et al. (2000) reported that the UPR facilitates the ER-associated protein degradation (ERAD), in which ER-accumulated misfolded proteins are retro-transported to the cytosol and subjected to the proteasomal degradation (Hiller et al., 1996). Moreover, cDNA microarray analyses revealed that the UPR induces genes encoding factors for protein transport across the ER and lipid-metabolism enzymes, as well as those encoding ER-located molecular chaperones, protein-folding enzymes and ERAD factors (Travers et al., 2000; Kimata et al, 2006). The UPR is thus likely to function for restoring and enhancing totally the ER functions. According to Fordyce et al. (2012), the *HAC1*$^{i}$ protein targets two different promoter elements, leading to the multiplicity of the UPR target genes. The *HAC1*$^{i}$ protein also contributes to transcriptional repression of the expression of some ER client proteins, which can possibly decrease protein load into the ER (Kimata et al., 2006). According to Niwa et al. (2004), the *HAC1* mRNA is the sole proximal target of Ire1 in *S. cerevisiae* cells.

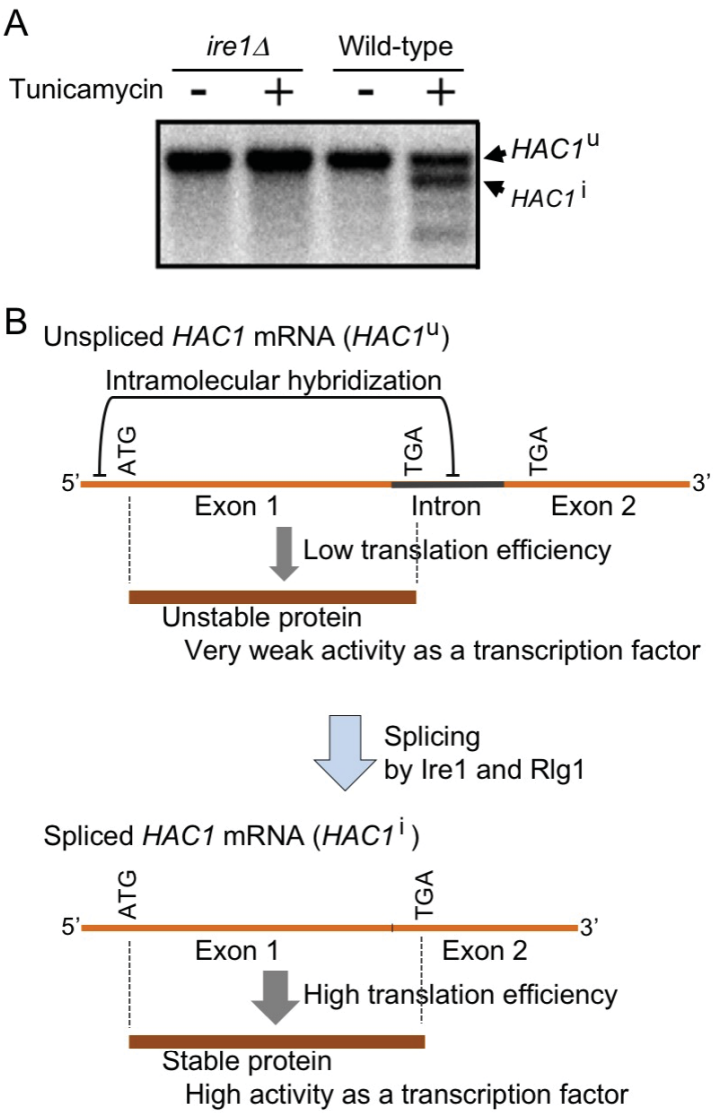


**Fig. 3 The *HAC1* mRNA is the target of yeast Ire1.**

(A) *IRE1*+ (wild-type) or *ire1Δ S. cerevisiae* cells were stressed by tunicamycin (2 μg/ml, 60 min) or remained unstressed. Their total RNA samples were then fractionated by electrophoresis and subjected to the Northern blot analysis to detect the *HAC1*-mRNA species. (B) The *HAC1* mRNA is spliced by Ire1 and Rlg1 in the cytoplasm.

### 1.2. Regulation of Ire1 in *S. cerevisiae* cells

Unlike the cytosolic domain, the luminal domain of Ire1 does not carry apparent functional motifs. Some experimental approaches were then employed to explore the structure-and-function relationship of the luminal domain of *S. cerevisiae* Ire1. Kimata et al. (2004) performed 10-a.a. deletion scanning of the luminal domain of Ire1, and proposed that it can be segmented into five subregions, namely Subregions I to V (Fig. 4A). While subregions II and IV are indispensable for Ire1's activity, the UPR was normally induced dependently on ER

stress when Ire1 carries a 10-a.a. deletion in Subregion I, III or V. In addition, Subregions I and V are quickly digested when the recombinant Ire1 luminal-region fragment is subjected to *in vitro* partial proteolysis (Oikawa et al., 2005). *In silico* analysis also predicted that Subregions I and V are intrinsically disordered (Fig. 4B; Mathuranyanon et al., 2015). Through the X-ray crystallographic analysis, Credle et al., (2005) exhibited the high-order structure of Subregions II to IV, which form one tightly folded module and thus named as the Core. Subregion III is a loosely folded loop sticking out from the Core (Fig. 4B).

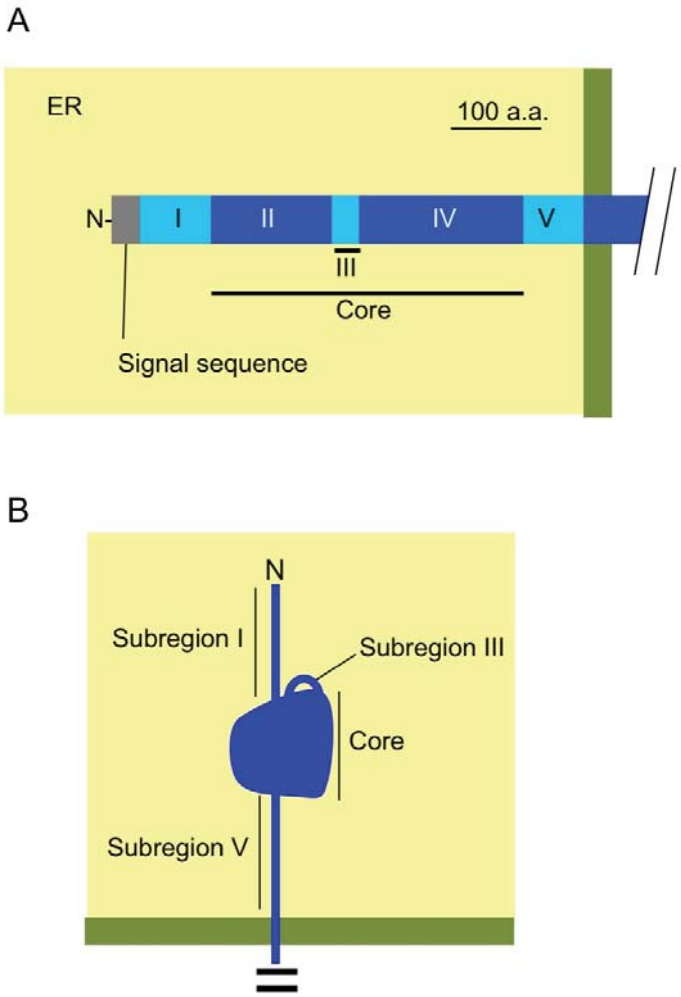


**Fig. 4 Structure of the luminal domain of yeast Ire1.**

(A) Kimata et al. (2004) propose to segment the luminal domain of *S. cerevisiae* Ire1 into five subregions (Subregions I to V). Subregions II and IV, but not I, III or V, are essential for Ire1's activity to splice the *HAC1* mRNA. (B) Structure of the luminal domain of *S. cerevisiae* Ire1 is schematically illustrated.

According to the X-ray crystal structure of the Core proposed by Credle et al. (2005), it can be self-associated via two different manners, resulting in its concatemer-like

oligomerization (Fig. 5A). Fig. 5B shows that Ire1 exhibits a dot-like distribution in ER-stressed *S. cerevisiae* cells, while Ire1 is diffusively distributed over the ER under unstress conditions. The Ire1 puncta are likely represent Core-dependent oligomerization, namely the cluster formation, of Ire1, since it is abolished by Ire1's point mutations which are deduced to impair the concatemer-like association of the Core (Kimata et al., 2007; Aragón et al. 2009). Ishiwata-Kimata et al. (2013)[a] reported that actin filaments contribute to the cluster formation of Ire1. Notably, such point mutants considerably impair evocation of the UPR (Kimata et al., 2007; Aragón et al. 2009). Thus it is highly likely that the cluster formation of Ire1 is required for Ire1's activation as an endoribonuclease. According to the X-ray crystal structural analysis of the cytosolic region of Ire1 reported in Korennykh et al. (2009), it exhibits a potent endoribonuclease activity when bundled. Aragón et al. (2009) and van Anken et al. (2014) demonstrated that the *HAC1*[u] mRNA is actively recruited to the Ire1 clusters for being spliced efficiently.

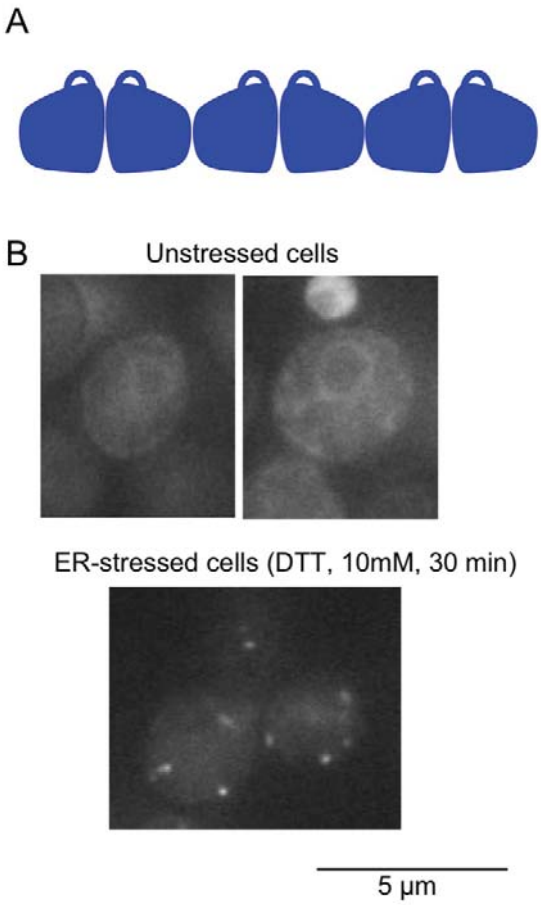


**Fig. 5 Cluster formation of yeast Ire1.**

(A) The Core intrinsically has an ability to form the high-order oligomer. (B) *S. cerevisiae* cells producing the fluorescent protein (mNeonGreen)-tagged Ire1 were observed under a fluorescent microscope.

Then how does ER stress lead to the cluster formation and activation of Ire1? Kohno et al. (1993) proposed that the UPR is suppressed in *S. cerevisiae* cells overproducing BiP, suggesting that BiP is a negative regulator of Ire1. According to Bertolotti et al. (2000) and Okamura et al. (2000), Ire1 is actually associated with BiP, which dissociates in response to ER stress. Yeast BiP mutants that cannot dissociate from Ire1 impair the UPR (Kimata et al, 2003), supporting the idea that association and dissociation between Ire1 and BiP controls the UPR. An *in vitro* reconstitution study argues that ER-accumulated unfolded proteins cause dissociation of the Ire1/BiP complex (Carrara et al., 2015).

Nevertheless, even if the BiP-binding site, namely Subregion V, is deleted, Ire1 is not constitutively activated, but is normally regulated dependently on ER stress (Kimata et al., 2004). This insight strongly suggests that the complex formation and its dissociation between Ire1 and BiP do not compose the main regulatory machinery for the UPR evocation in response to ER stress. The X-ray crystal structure of the Core demonstrated that its dimer forms a cavity to which stretched peptides may be captured (Credle et al., 2005). *In vitro* analyses performed in Kimata et al. (2007) and Gardner and Walter (2011) demonstrated physical interaction between the recombinant Core protein and model unfolded peptides. Moreover, Ire1 appears to actually associates with misfolded proteins accumulated in the ER of *S. cerevisiae* cells (Gardner and Walter, 2011; Promlek et al., 2011). According to Kimata et al. (2007) and Promlek et al. (2011), full length deletion of Subregion III, namely the ΔIII mutation, of Ire1 impairs the *in vitro* and *in vivo* physical association between Ire1 and misfolded proteins. Because the ΔIII mutation impairs the UPR evocation in response to ER-accumulation of misfolded proteins, it is highly likely that capturing of misfolded proteins by the Core leads to activation of Ire1 (Kimata et al., 2007; Promlek et al., 2011). Gardner and Walter (2011) proposed that physical interaction between misfolded proteins and the Core bundles Ire1.

Fig. 6 represents the current model that explain the molecular mechanism by which Ire1 senses ER-accumulated misfolded proteins and is activated. Under nonstress conditions, BiP is associated with Ire1, which then remains non-self-associated. Meanwhile, misfolded proteins accumulated in the ER deprives Ire1 of BiP, and is captured by Ire1, which is then clustered and activated. According to Oikawa et al. (2007) and Mathuranyanon et al. (2015), Subregion I also contributes to repression of the UPR. Subregion I appears to be intramolecularly captured by the Core, contributing to suppression of Ire1's activity, under nonstress conditions.

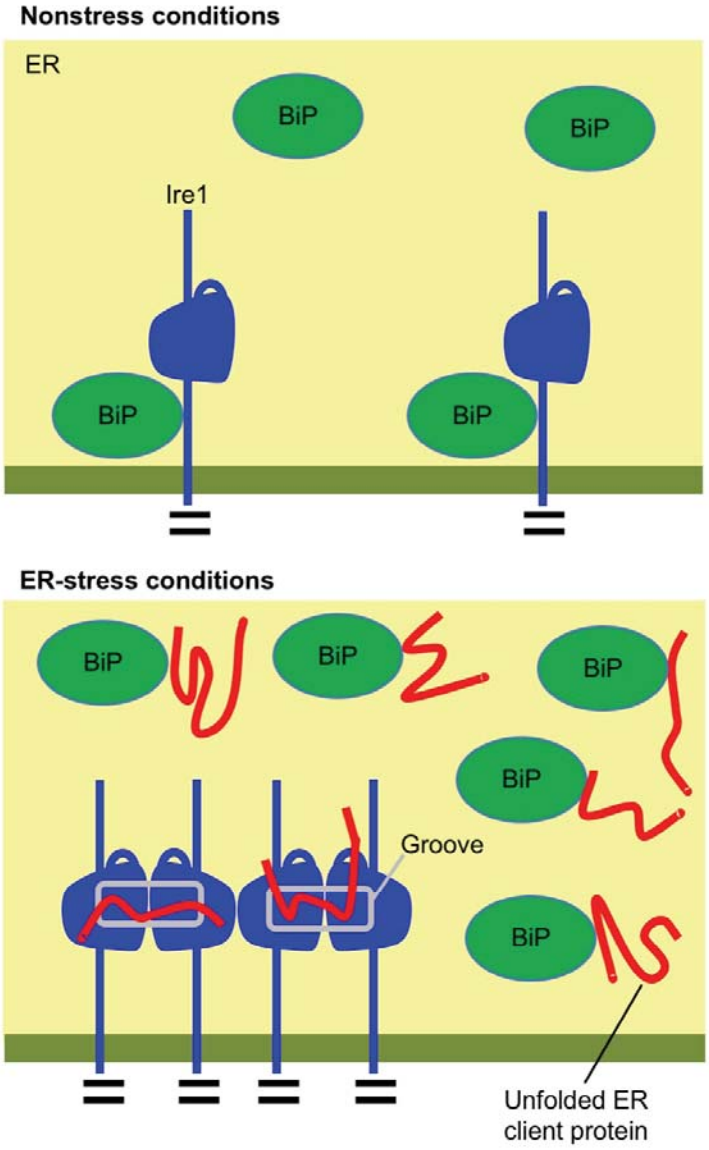


**Fig. 6 Molecular mechanism by which ER-accumulated unfolded proteins promotes the cluster formation and activation of yeast Ire1.**

In non-stressed *S. cerevisiae* cells, BiP is associated with Ire1, which then remains non-self-associated. Meanwhile, under ER stress conditions, BiP is dissociated from Ire1, which then captures unfolded proteins and forms the clusters that exhibit strong endoribonuclease activity.

When *S. cerevisiae* cells are suffered from a moderate level of ER stress that is not deadly strong, the UPR is attenuated after its peak induction (Pincus et al., 2010; Chawla et al., 2011; Rubio et al., 2011). Chawla et al. (2011) and Rubio et al. (2011) reported that the UPR is sustainably induced even under the recovery phase from ER stress in cells carrying Ire1 mutants that can be activated without being auto-phosphorylated. Notably, cell survival upon ER stress is diminished by these Ire1 mutations, suggesting importance of the

dephosphorylation of Ire1 for UPR attenuation and cell survival after peak induction of the UPR. Re-association of BiP with Ire1 also contributes to downregulation of Ire1 after its peak activation, since Subregion V-deletion mutants of Ire1 not carrying the BiP-binding site exhibit impaired attenuation of its activity (Pincus et al., 2010; Ishiwata-Kimata et al., 2013[b]). By considering that BiP is transcriptionally induced through the UPR, Ire1's regulation by BiP is likely to a negative feedback loop.

### 1.3. Scenes in which the UPR functions in *S. cerevisiae* cells

For laboratory studies on the UPR of *S. cerevisiae*, ER stress have been induced, for example, through exposure of cells to the N-glycosylation-inhibiting antibiotic tunicamycin or the disulfide-bond cleaving agent dithiothreitol (DTT) or exogenous expression of model misfolded proteins. Then, under what conditions other than these laboratorial and artificial stressing stimuli does Ire1 function in *S. cerevisiae* cells?

*S. cerevisiae* is industrially used for ethanol fermentation very frequently. According to Miyagawa et al. (2014), ethanol stress leads to protein denaturing and aggregation in the ER, and then results in activation of Ire1 and in evocation of the UPR. In addition, bioethanol production from lignocellulosic biomass is accompanied with accumulation of acetic acid, which also induces ER stress and the UPR (Kawazoe et al., 2017). Le et al. (2016) reported that an environment-polluting metal ion cadmium impairs protein folding in the ER, and that the UPR is involved in cellular survival against cadmium stress.

Stressing stimuli that appear to predominantly impair membrane-lipid integrity also activate Ire1 and evoke the UPR in *S. cerevisae* cells. Intriguingly, such conditions, which include inositol depletion (Cox et al., 1997) and mutations of genes involved in lipid biosynthesis, activate wild-type Ire1 and ΔIII Ire1 almost equally (Promlek et al., 2011). It is thus likely that Ire1 senses membrane-lipid aberrancy in a manner which is different from that for sensing of ER-accumulated misfolded proteins. Halbleib et al. (2017) proposed that the transmembrane domain of Ire1 is responsible for sensing of membrane-lipid aberrancy by Ire1.

### 1.4. Aim and findings of this study

As described above, the yeast Ire1-*HAC1* pathway of the UPR transcriptionally induces a number of genes including those encoding not only ER-located molecular chaperones and protein-folding enzymes but also enzymes to generate membrane-lipid components and to remove reactive oxygen species (ROS) (Cox et al., 1997; Travers et al., 2000; Kimata et al., 2006). Moreover, membrane-lipid aberrancy is likely to activate Ire1 independently of accumulation of unfolded proteins in the ER (Promlek et al., 2011; Volmer et al., 2013;

Halbleib et al., 2017). The UPR thus seems to function not only for coping with ER accumulation of unfolded proteins, and I have therefore searched for new scenes in which the UPR works in yeast cells.

When inoculated into a medium rich in fermentable sugar, such as glucose, yeast cells are fueled from its fermentation for rapid growth. Cell growth is then retarded upon exhaustion of the fermentable sugar, as cells utilize the fermentation products as carbon and energy source through respiration. This switch from anaerobic growth to aerobic respiration is called the diauxic shift, which is accompanied by a drastic change of the gene expression profile and by massive expansion of the mitochondria (DeRisi et al., 1997; Egner et al., 2002; Ohlmeier et al., 2004). Here I report UPR induction in yeast cells upon the diauxic shift and during their cultivation in a non-fermentable medium without external stressing stimuli. Intriguingly, in this case, Ire1 is likely to be activated not by ER-accumulated unfolded proteins but by ROS. I also note the involvement of this phenomenon in expansion of the mitochondria.

# CHAPTER II
# MATERIALS AND METHODS

## 2.1. Yeast culturing

Unless otherwise noted, yeast cells were cultured in SD medium containing 2% glucose, 0.66% yeast nitrogen base without amino acids (YNB w/o A.A.; Difco) and appropriate auxotrophic requirements. YPD medium contains 1% yeast extract (Bacto), 2% Peptone (Bacto) and 2% glucose. To support cellular growth in synthetic glycerol medium containing 5% glycerol and 0.66% YNB w/o A.A., I supplemented it with the standard histidine-dropout complete pre-mix, which is composed of 2.0 g each of 18 proteinogenic amino-acid powders (all standard proteinogenic amino acids excluding leucine and histidine), 10.0 g of leucine, 0.5 g of adenine, 2.0 g of uracil and 2.0 g of *p*-aminobenzoic acid, at a final concentration of 2.0 g/L (SCGlycerol).

Unless otherwise noted, throughout this study, cells were overnight shaken at 30°C in a liquid medium, and the resulting pre-cultures were diluted in the same medium (setting $OD_{600}$ of 0.30) and further shaken aerobically at 30°C. In the experiments shown in Figs 7E and F, overnight YPD pre-cultures were 1 to 10 diluted with YPD medium for further culturing at 30°C. In the experiment shown in Figs 14A and B, cells under the exponential and fermentative growing phase in SD medium were washed with SCGlycerol medium for three times by repeated centrifugation and resuspension before being cultured in SCGlycerol medium. A spectrophotometer SmartSpec Plus (BioRad) was used to measure optical density at 600 nm of cultures.

## 2.2. Yeast strains and plasmids

Unless otherwise noted, I employed strains derived from W303-ire1Δ (*MAT**a** ura3-1 trp1-1 leu2-3,112 his3-11,15 ADE2 ire1::TRP1 can1-100*; Le et al., 2016) throughout this study. Another stain KMY1005 (*MATΔ leu2-3,112 ura3-52 his3Δ200 trp1Δ901 lys2-801*; Mori et al., 1996) was employed in the experiment shown in Fig. S3. KMY1516 (*MATΔ LEU2::UPRE-GFP LYS2::UPRE-lacZ ura3-52 his3Δ200 trp1Δ901 ire1::TRP1*; Kimata et al, 2004) is a derivative of KMY1005 and was used in the experiments shown in Figs 8, 12C, 12D and 13D.

To generate *IRE1*+ cells, I transformed W303-ire1Δ or KMY1516 with pRS313-IRE1 (Kimata et al, 2004), which is a centromeric plasmid carrying the *IRE1* gene (the coding sequence plus the 5'- and 3'-untranslated regions). A centromeric plasmid that was used for expression of the C-terminally HA-tagged version of Ire1 (Ire1-HA), pRS315-IRE1-HA, is

also referred in a previous publication (Kimata et al, 2004). Partial-deletion and point mutations of the *IRE1* gene were introduced into pRS313-IRE1 or pRS315-IRE1-HA by using the overlap-PCR and *in vivo* homologous-recombination techniques (Kimata et al., 2004). A similar procedure was employed for introduction of the bZIP mutation into pRS313-IRE1 or pRS315-IRE1-HA as described previously (Promlek et al., 2011). W303-ire1Δ transformed with an empty vector pRS313 (Sikorski and Hieter, 1989) were used as *ire1Δ* cells. For cellular expression of eroGFP and mitochondria-localized GFP, we respectively used plasmids pPM28 and pYX142-mtGFP (Merksamer et al., 2008; Westermann and Neupert, 2000).

To generate a *hac1Δ* strain W303-hac1Δ, W303-ire1Δ transformed with pRS313-IRE1 was further transformed with the *hac1::KanMX4* gene-disruption module, which had been PCR amplified from a EUROSCARF gene disruption-library strain. To introduce the $\rho^0$ mutation, cells were overnight cultured in YPD medium containing 10 $\mu$g/ml ethidium bromide, and clones that cannot grown on the glycerol-based medium were selected.

In order to express quantified numerical data throughout this report, I obtained the average values with standard deviations from results from multiple (mostly three) independent transformant clones carrying the same plasmid (pRS313, pRS313-IRE1 or its mutants).

### 2.3. Chemicals

DTT (Nacalai Tesque), tunicamycin (Sigma Aldrich), antimycin A (Sigma Aldrich) and NAC (Sigma Aldrich) were respectively prepared as stock solutions of 1 M in water, 2 mg/ml in dimethyl sulfoxide (DMSO), 20mM DMSO and 0.5 M in water, and stored at -30°C. Hydrogen peroxide was obtained as a 35% water solution (Nacalai Tesque). For chemical-stress imposition, DTT, tunicamycin or hydrogen peroxide was added into cultures on the exponential and fermentative growing phase.

### 2.4. RNA and DNA analyses

The hot phenol method was used for extraction of total RNA from yeast cells (Kimata et al., 2003). As described previously (Promlek et al., 2011), the RNA samples were subjected to RT-PCR amplification of the *HAC1* transcripts using the polyA RT primer and the *HAC1*-specific PCR primers (Table 1). The PCR products were then analyzed by 2% agarose-gel electrophoresis (TBE buffer), and ethidium bromide-fluorescent images of the resulting gels were pictured with the GelDoc XR+ imaging system (BioRad) and are presented in Figs 7A, 7C and S3. Alternatively, the gel images were subjected to image quantification, the results of which were used to obtain the values of the *HAC1* splicing efficiency through the formula of

[(band intensity of *HAC1*$^{i}$)/{(band intensity of *HAC1*$^{i}$)+(band intensity of *HAC1*$^{u}$)}], where *HAC1*$^{i}$ and *HAC1*$^{u}$ respectively are the spliced and unspliced forms of the *HAC1* mRNA.

**Table 1** Oligonucleotide primers for RT-PCR, qPCR or RT-qPCR

| Target gene | | Sequence |
|---|---|---|
| *HAC1* | Forward | TACAGGGATTTCCAGAGCACG |
| | Reverse | TGAAGTGATGAAGAAATCATTCAATTC |
| *KAR2* | Forward | TCTGAAGGTGTCTGCCACAG |
| | Reverse | TTAGTGATGGTGATAGATTCGGATT |
| *PDI1* | Forward | TACGAAGAAGCCCAGGAAAA |
| | Reverse | GTCAGCCAATTCAGCGTCA |
| *TSA1* | Forward | GTTCATCATCGACCCAAAGG |
| | Reverse | GTCAACGTTTCTACCGACTGG |
| *OLI1* | Forward | GCAGGTATTGGTATTGCTATCG |
| | Reverse | GCTTCTGATAAGGCGAAACC |
| *TAF10* | Forward | ATATTCCAGGATCAGGTCTTCCGTAGC |
| | Reverse | GTAGTCTTCTCATTCTGTTGATGTTGTTGTTG |

In order to remove residual genomic DNA from the total RNA samples before real-time RT-qPCR analysis and high-throughput RNA-seq analysis, I treated them with recombinant DNase I (RNase-free; Takara) as indicated by manufacturer's instruction. For the RT-qPCR analysis, the resulting total RNA samples were subjected to the RT reaction as done in the case of the RT-PCR amplification of the *HAC1* transcripts. Then the RT-reaction products were analyzed with SYBR Premix Ex Taq™ II (Tli RNaseH Plus; Takara) and the real-time PCR machine LightCycler 96 (Roche). The quantitative PCR (qPCR) condition was as follows; pre-incubation: 95 °C 5 min, and 3-step cycle amplification: 95°C 10 sec/60°C 10 sec/72°C 10 sec. Primer sets used in this analysis are listed in Table 1. The *TAF10* primer sets served as the internal control.

Genomic DNA was extracted from yeast cells using GenTLE yeast DNA extraction kit (Takara) and analyzed by the qPCR technique.

Preparation of next generation sequencing (NGS) libraries and NGS were performed at the Eurofins genomics K.K. (Tokyo) under the following conditions: sequencer: HiSeq2500 (Illumina), read length: 125 bases of paired-end, software: bclfastq2 software v1.8.4 (Illumina). The NGS data were deposited in ArrayExpress (https://www.ebi.ac.uk/arrayexpress/;

accession E-MTAB-6923). After NGS analysis, fastq files were processed for trimming, filtering and mapping with CLC genomic work bench v10.1(Qiagen) under the default setting. The processed NGS data were mapped on *Saccharomyces cerevisiae* S288C genome version R64-1-1. Based on the mapped data, TPM as gene expression values were calculated with CLC genomic work bench v10.1.

**2.5. Protein analysis**

As described in Kimata et al. (2003) and Mai et al. (2018), yeast cells were broken by agitation with glass beads in the lysis buffer containing 50mM Tris-Cl (pH7.9), 5mM ethylenediaminetetraacetic acid, 1% Triton X-100 and protease inhibitors, and the resulting crude cell lysates were clarified by centrifugation at 8,000 Xg for 10 min. For the BiP sedimentation assay, crude cell lysates were sequentially centrifuged at 700 Xg for 3 min and at 8000 Xg for 20 min. Then the pellet fractions obtained through the second centrifugation were further analyzed as the "pellet" samples in the experiment shown in Fig. 11A. Western blot analyses using anti-HA, anti-BiP and anti-Pgk1 antibodies were performed as described previously (Kimata et al., 2003; Mai et al., 2018). Mouse monoclonal antibody 6G9E6BC4 (Abcam) was used for Western-blot detection of Por1.

**2.6. Microscopic analysis**

In order to obtain fluorescent images of eroGFP, yeast cells transformed with pPM28 were observed under the microscope Keyence BZ-9000E carrying the objective lens CFI Plan Apo λ100xH (Nikon). I used the fluorescence filter set OP-79301 for excitation with blue light (1.0 sec exposure) and a custom-made fluorescence filter set (excitation wavelength 395/25, dichroic mirror wavelength 495, emission 510/20) for excitation with UV/violet light (1.3 sec exposure). Then, ratio of the signal intensities under the blue-light excitation and that under the UV/violet-light excitation of each cell was obtained using the image processing software Image J (https://imagej.nih.gov/ij/). At least 30 cells were analyzed for one culture sample.

To check cellular survival, I resuspended harvested cells in PBS containing 1 $\mu$M/ml propidium iodide (PI) for 30 min, and observed them under the same fluorescent microscope (filter set OP-79302) for counting the numbers of PI-stained and unstained cells. At least 100 cells were counted for one culture sample.

In order to obtain fluorescent images of mitochondria-located GFP, cells transformed with pYX142-mtGFP were observed using a confocal laser scanning microscope LSM700 (Zeiss) carrying a Plan-Apochromat 100x/1.40 objective lens (Zeiss) under the condition of a pinhole 0.74 airy unit, argon laser 100% output and the EGFP smart-setup and auto-expose

mode. We obtained a confocal fluorescent image (512X512 pixels, zoom 2.4) after focusing on the center of a cell, which was then binarized by using Image J (default setting) for measuring of its mitochondria area. In the experiment shown in Fig. 16C, approximately 100 cells (the mother cell in the case of a budded cell) were analyzed for their mitochondria area on each sample.

**2.7. Flow cytometry**

After addition of 2', 7'-Dichlorodihydrofluorescin diacetate (DCDHF-DA, 2.5 $\mu$g/ml final concentration) into cultures and further incubation for 30 min, cells were analyzed by the flow cytometer Accuri C6 (BD Biosciences). FL1 (530/630 nm) fluorescence data from DCDHF-DA stained cells were normalized against the mean FL1 values of unstained cells.

**2.8. Oxygen consumption monitoring**

MitoXpress Xtra (Luxcel Biosciences) is constituted from a fluorophore ($Ex_{min}$: 380 mM and $Em_{max}$: 650 nm), the fluorescence of which is quenched by dissolved oxygen. After being aerated by 1-min top-speed vortexing, 300 $\mu$L of post-diauxic-shift culture was quickly mixed with 25 $\mu$L of the MitoXpress Xtra solution and put into a quarts cell, which was then sealed by mineral oil, for measurement with a fluorescence spectrophotometer F-7000 (Hitachi; excitation: 380 nm, slit width: 5 nm, photomultiplier: 950 nm). Fluorescent intensities were monitored every 15 sec, and the net fluorescence at each time point was obtained by the formula of [(fluorescent intensity at 650 nm) – (fluorescent intensity at 675 nm (background))]. After normalizing the net fluorescence by the formula of [{(the net fluorescence at a time point) – (the minimum net fluorescence)} / {(the maximum net fluorescence) – (the minimum net fluorescence)}], we obtained the relative oxygen consumption rate (per culture density) via the following formula;

1 / {(duration from the time point at which the normalized net fluorescence reaches 35% of the maximum to the time point at which the normalized net fluorescence reaches 80% of the maximum) X ($OD_{600}$ culture density)}.

# CHAPTER III
# RESULTS

## 3.1. The Ire1-*HAC1* signaling pathway of the UPR is activated upon diauxic shift of yeast cells.

This research has begun from my finding that a considerable but transient UPR is observed upon long-time culturing of yeast cells in standard synthetic dextrose (SD) medium. Unless otherwise noted, throughout this study, my yeast strains were overnight incubated in SD medium, and then the resulting pre-cultures were diluted with the same medium (setting $OD_{600}$ of 0.30) for further culturing and time-course harvesting. Fig. 7A and its quantification data shown in Fig. 7B indicate a transient induction of the *HAC1*-mRNA splicing in *IRE1*+ cells cultured through this procedure. This phenomenon seems to accompany diauxic shift, since after this time point (8-hr after culture start), cells grew slowly (Fig. 7C) and accumulated reactive oxygen species (ROS; Fig. S1), which are byproducts of aerobic respiration. Fig. S2 exhibits a more detailed time-course profile of the transient induction of the *HAC1* mRNA splicing.

As well as in the case of canonical ER-stressing stimuli, the *HAC1*-mRNA splicing shown in this study is caused by Ire1, since no *HAC1*-mRNA splicing was observed in cells not carrying the *IRE1* gene (the *ire1Δ* mutation) even when they reached diauxic shift (Fig. 7D, see Fig. 10A for growth profile of *ire1Δ* cells). As shown in Fig. S3, another *IRE1*+ strain that is not congenic with the strains used throughout this study similarly exhibited a transient *HAC1*-mRNA along long-time culturing. A transient *HAC1*-mRNA splicing upon end of the exponential cell growth was also observed when cells were grown in the rich yeast extract-peptone-dextrose (YPD) medium (Figs 7E and F). Western-blot detection of the hemagglutinin (HA)-epitope tagged Ire1 indicates that the cellular level of Ire1 is almost unaffected through the culturing procedure employed in this study (Fig. 8).

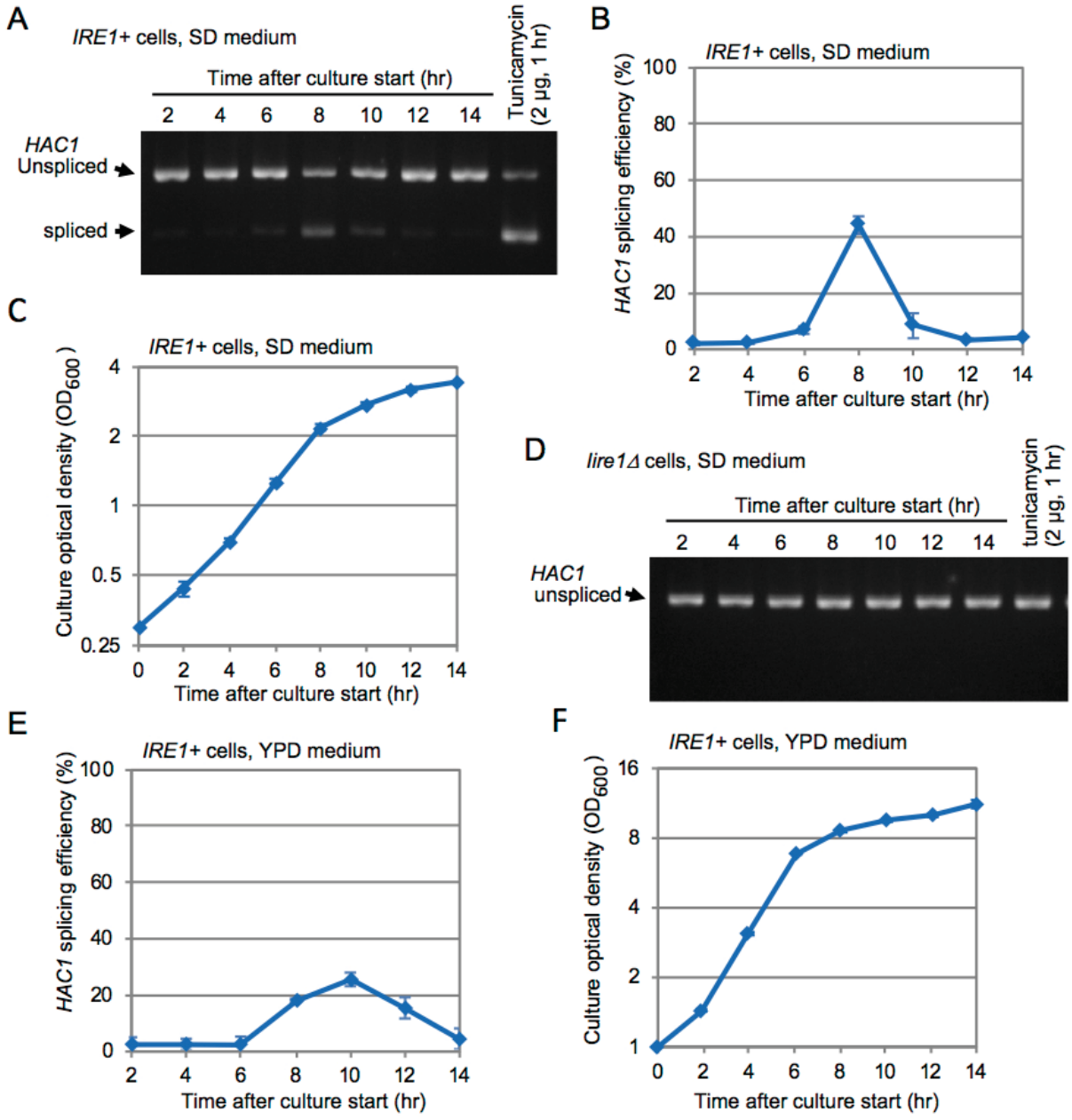


**Figure 7: *HAC1*-mRNA splicing is transiently induced upon diauxic shift of yeast cells.**

(A) After being cultured for the indicated durations in SD medium or stressed by the canonical ER stressor tunicamycin, *IRE1*+ cells were checked for RT-PCR amplification of the *HAC1* transcripts. (B) The same experiment as shown in panel A were performed using three independent clones of *IRE1*+ cells to obtain quantified data. (C) Optical density of the cultures analyzed in panel B is presented. (D) The same experiment as done in panel A were performed using *ire1Δ* cells. (E) and (F) *IRE1*+ cells were cultured in YPD, and checked for the *HAC1*-mRNA splicing and culture density.

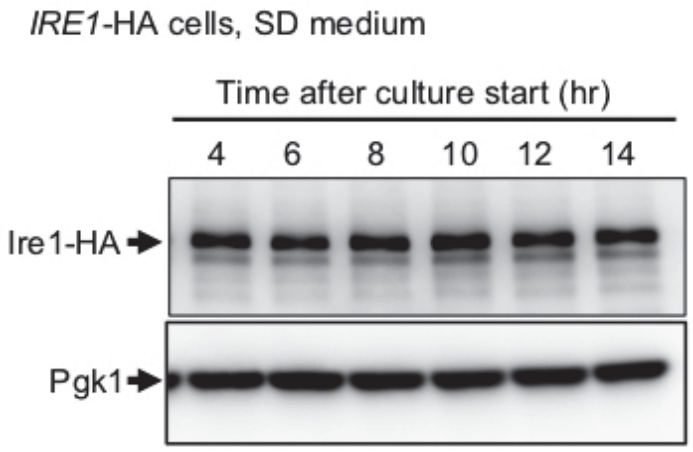


**Figure 8: Time-course change of the cellular Ire1 level.** Cells carrying Ire1-HA were cultured in SD medium for the indicated durations. Then their lysates (equivalent to 2.5 OD600 cells) were subjected to anti-HA Western-blot analysis. Anti-Pgk1 Western blot serves as a loading control.

### 3.2. The linkage between mitochondrial respiration and transient induction of the UPR

The $\rho^o$ mutation of yeast cells is a loss of the mitochondrial genome and is known to abolish aerobic respiration. According to my data shown in Fig. S1B, ROS level in $\rho^0$ cells which reached a growth-retardation phase (Fig. 9A) is not seemingly different that of fermentatively growing wild-type cells. As shown in Figs 9A and B, the *HAC1*-mRNA splicing upon end of the exponential and fast cell growth was only faint in $\rho^o$ mutant cells. This observation supports my idea that the transient induction of the *HAC1* splicing observed in this study is tightly linked to diauxic shift, which accompanies induction of mitochondrial respiration. In order to demonstrate the relationship between mitochondria function and Ire1 activation upon diauxic shift, we next used a mitochondria inhibitor antimycin A. In the experiment shown in Figs 9C, D, and S1C, *IRE1*+ cells were cultured in the presence of 20 $\mu$M/ml antimycin A, which did not affect cellular growth, but did impair the *HAC1*-mRNA splicing upon diauxic shift and lower ROS production.

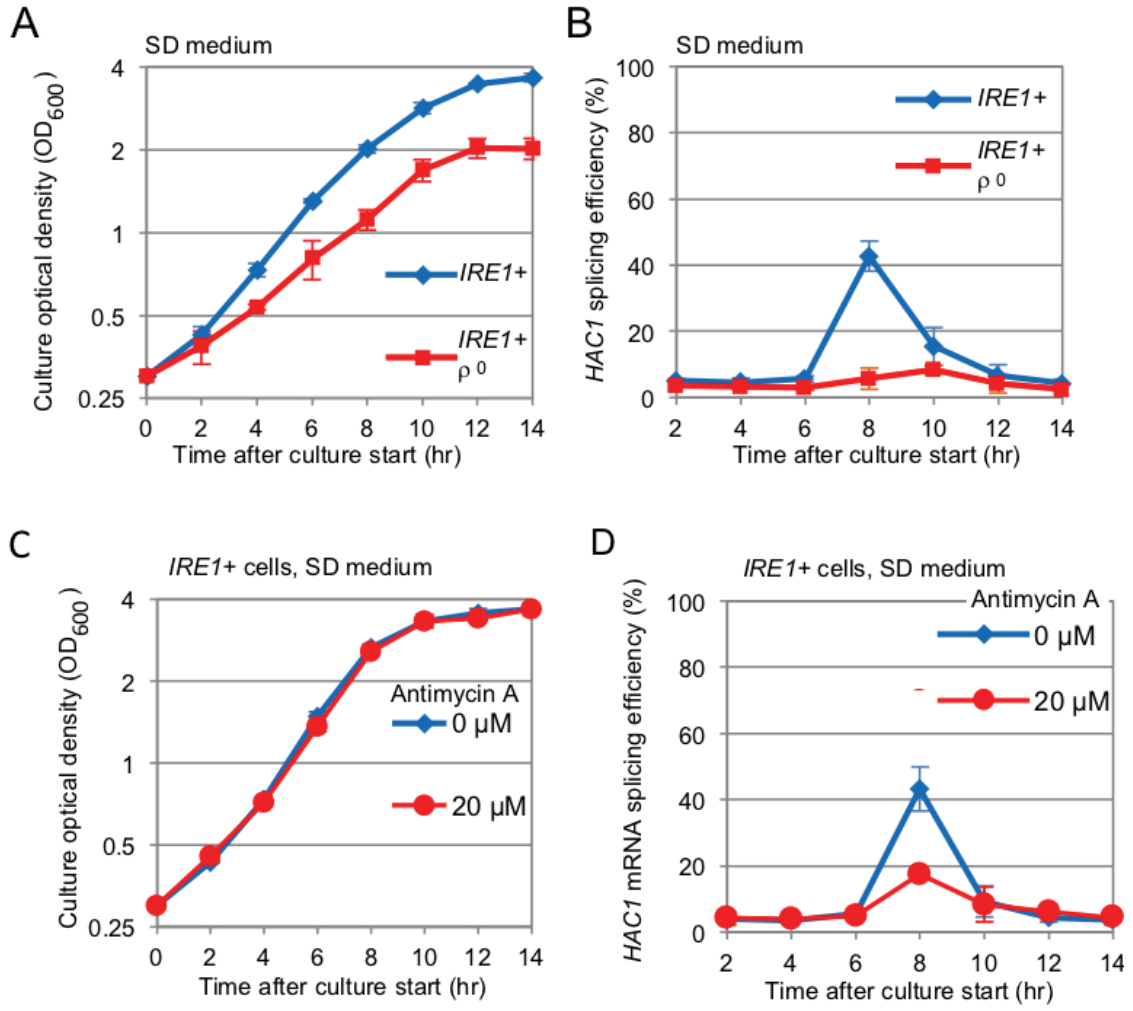


**Figure 9: The ρ⁰ mutation and antimycin A impair the *HAC1*-mRNA splicing upon diauxic shift.** (A) and (B) The same experiments as done in Figs 7B and C were performed using *IRE1*+ cells and its ρ⁰ mutant. (C) and (D) Antimycin A was added into culture at time 0, and the same experiments as described in Figs 7B and C were performed.

### 3.3. The contribution of Ire1-*HAC1* pathway to cellular growth and survival after diauxic shift.

I next asked a contribution of Ire1 to growth of cells that reached diauxic shift. In the experiment shown in Fig. 10A, I compared growth of *IRE1*+ cells and that of *ire1Δ* cells, and found that the *ire1Δ* mutation retards cellular growth after diauxic shift (8-hr after culture start). My observation shown in Fig. 10B indicates that the *hac1Δ* mutation caused a similar growth retardation as the *ire1Δ* mutation, suggesting that, as well as in the case of cellular response against canonical ER stressing stimuli, Ire1 and *HAC1* work proximately for cellular growth after diauxic shift. Cellular survival after diauxic shift was also impaired by the *ire1Δ* mutation (Fig. 10C)

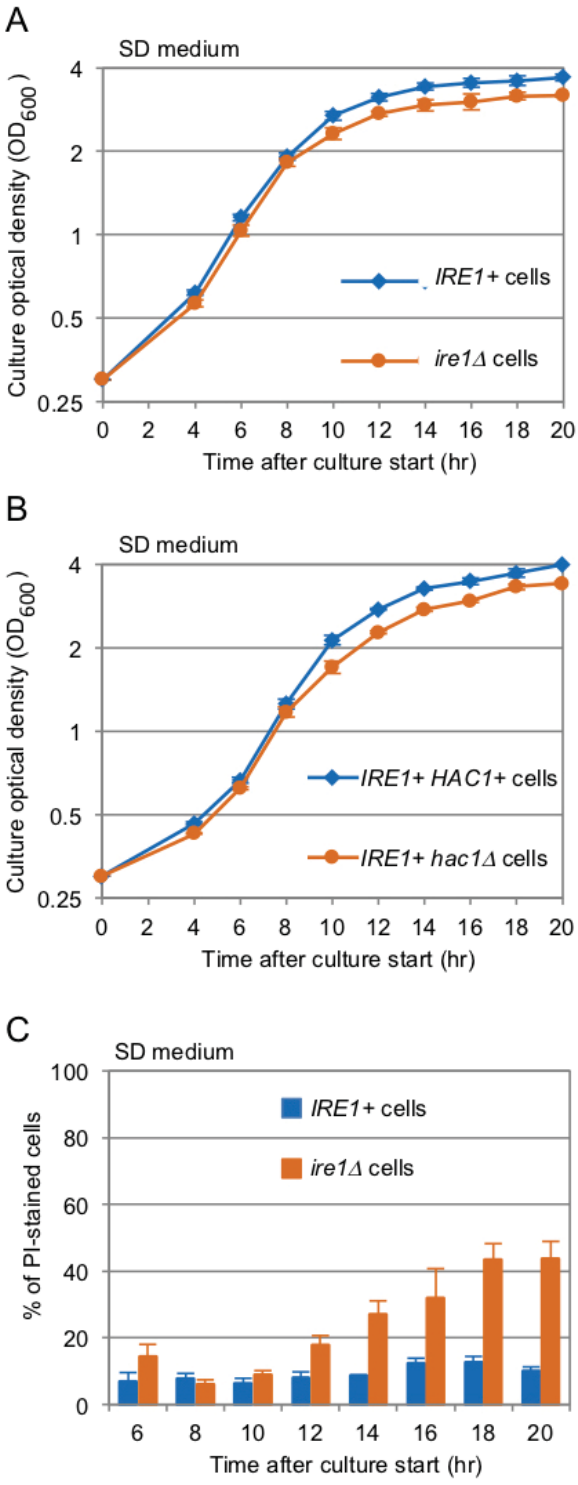


**Figure 10: The Ire1-*HAC1* pathway contributes to cellular growth and survival after diauxic shift.** (A) and (B) Cells were grown in SD media, and optical density of cultures at the indicated time points was monitored. (C) After being cultured in SD media for the indicated durations, cells were stained with PI and observed under fluorescent microscope for checking ratios of PI-stainable dead cells.

### 3.4. ER protein folding is not impaired upon diauxic shift of yeast cells.

In general, Ire1 is thought to exert a potent *HAC1*-mRNA splicing activity through sensing ER accumulation of unfolded proteins (Kimata and Kohno, 2011). Then, is protein folding in the ER damaged upon diauxic shift of yeast cells?

In the experiment shown in Fig. 11A, I performed the BiP sedimentation assay (Promlek et al., 2011; Nguyen et al., 2013; Miyagawa et al., 2014; Le et al., 2016), through which I can estimate production of ER protein aggregates that incorporate BiP. In this assay, cell lysates were fractionated by centrifugation before being analyzed by anti-BiP Western blotting. Both cellular treatment with dithiothreitol (DTT), which is a disulfide-bond reducing reagent, and diauxic shift serves as a potent and conventional ER stressor, slightly increased the BiP abundance in total cell lysates, since BiP expression is transcriptionally induced by the Ire1-*HAC1* pathway of the UPR. However, only the former stimulus drastically increased the BiP level in the pellet fraction, which represents the abundance of unfolded-protein aggregates in the ER.

I next employed yeast cells expressing eroGFP, which is an ER-located version of GFP and changes its excitation spectrum dependently on its intramolecular disulfide-bond formation (Merksamer et al., 2008). As shown in Fig 11B, DTT treatment of cells, but not diauxic shift, considerably changed the excitation spectrum of eroGFP, suggesting that diauxic shift does not significantly disturb disulfide bond-forming ability of the yeast ER.

In order to provide another line of evidence for my idea that diauxic shift activates Ire1 without ER accumulation of unfolded proteins, I employed a partial deletion mutant of Ire1, namely ΔIII Ire1 (Fig. S4), which is impaired in sensing of unfolded proteins (Kimata et al., 2007; Promlek et al., 2011). Importantly, while insufficiently activated by unfolded proteins accumulated in the ER (Kimata et al., 2007), ΔIII Ire1 is likely to trigger the UPR to an almost equal extent with wild-type Ire1 in response to certain stressing stimuli (Promlek et al., 2011). Figs 12A and B indicate that cells carrying ΔIII Ire1 exhibited an almost identical *HAC1* mRNA-splicing profile as wild-type Ire1 cells upon diauxic shift.

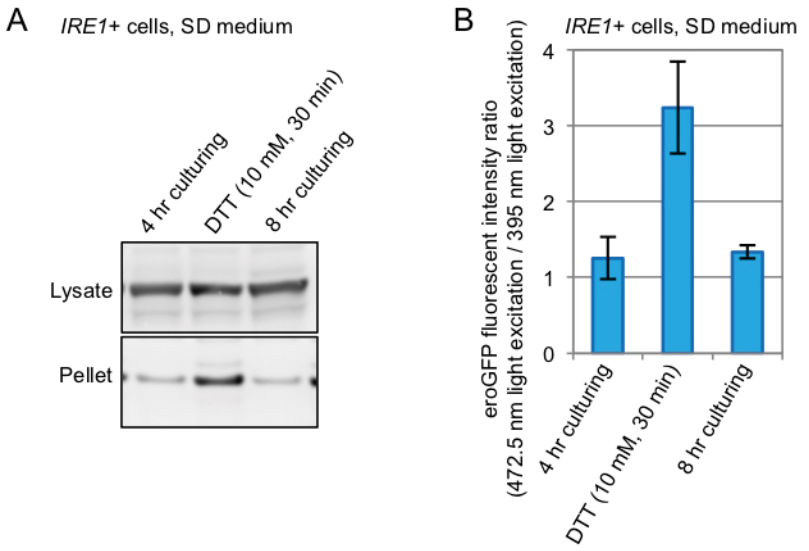


**Figure 11: Protein-folding status is not impaired upon diauxic shift.**

After being cultured for the indicated durations or stressed by DTT, *IRE1*+ cells were lysed and subjected to high-speed centrifugation as described in the Materials and Methods section. Then the total cell lysates (equivalent to 0.05 OD600 cells) or the pellet fractions (equivalent to 2.5 OD600 cells) were subjected to anti-BiP Western-blot analysis. (B) After being cultured for the indicated durations or stressed by DTT, *IRE1*+ cells producing eroGFP were illuminated by UV/violet light or blue light under a fluorescent microscope to observe green fluorescent signal.

### 3.5. Regulatory roles of domains of Ire1 for its transient activation upon diauxic shift.

In order to approach the regulatory mechanism of Ire1 upon diauxic shift, I further employed yeast cells carrying luminal-domain mutants of Ire1, which are illustrated in Fig. S4. The bZIP mutation of Ire1 is a replacement of its full-length luminal domain to a dimer-forming basic leucine-zipper (bZIP) peptide that is derived from a nuclear transcription factor protein Gcn4 (Promlek et al., 2011). As shown in Figs 12C and D and reported previously (Promlek et al., 2011), bZIP-Ire1 cells exhibited a considerable *HAC1*-mRNA splicing even when exponentially and fermentatively growing, since bZIP-Ire1 is constitutively self-associated through its bZIP domain. Importantly, splicing of the *HAC1* mRNA in bZIP-Ire1 cells was further stimulated upon diauxic shift, and, unlike to the case of wild-type *IRE1* cells, was not attenuated on the post diauxic-shift phase (Figs 12C and D). I thus speculate that an activation signal works to the cytosolic (or transmembrane) domain of Ire1 for the UPR evocation upon diauxic shift. Nevertheless, the luminal domain of Ire1 also seems to contribute to the regulation of Ire1 in this case, since wild-type Ire1 but not bZIP-Ire1 was downregulated after diauxic shift.

According to previous reports (Kimata et al., 2004; Pincus et al., 2010; Mathuranyanon et al., 2015), the luminal domain of Ire1 carries two subregions, namely N-terminal Subregion I and juxtamembrane-positioned Subregion V (Fig. S4), which contribute to downregulation of Ire1. I then asked contribution of these subregions to regulation of Ire1 for the transient evocation of UPR upon diauxic shift. Confirming a previous report (Oikawa et al., 2007), cells carrying deletions of both Subregions I and V (the ΔIΔV mutation) exhibited a substantial *HAC1* mRNA splicing even when growing exponentially and fermentatively (Figs 12E and F). Here I note transient stimulation of the *HAC1* mRNA splicing upon diauxic shift in ΔIΔV Ire1 cells, which implies that neither Subregion I nor V plays important role for regulation of Ire1 in this case.

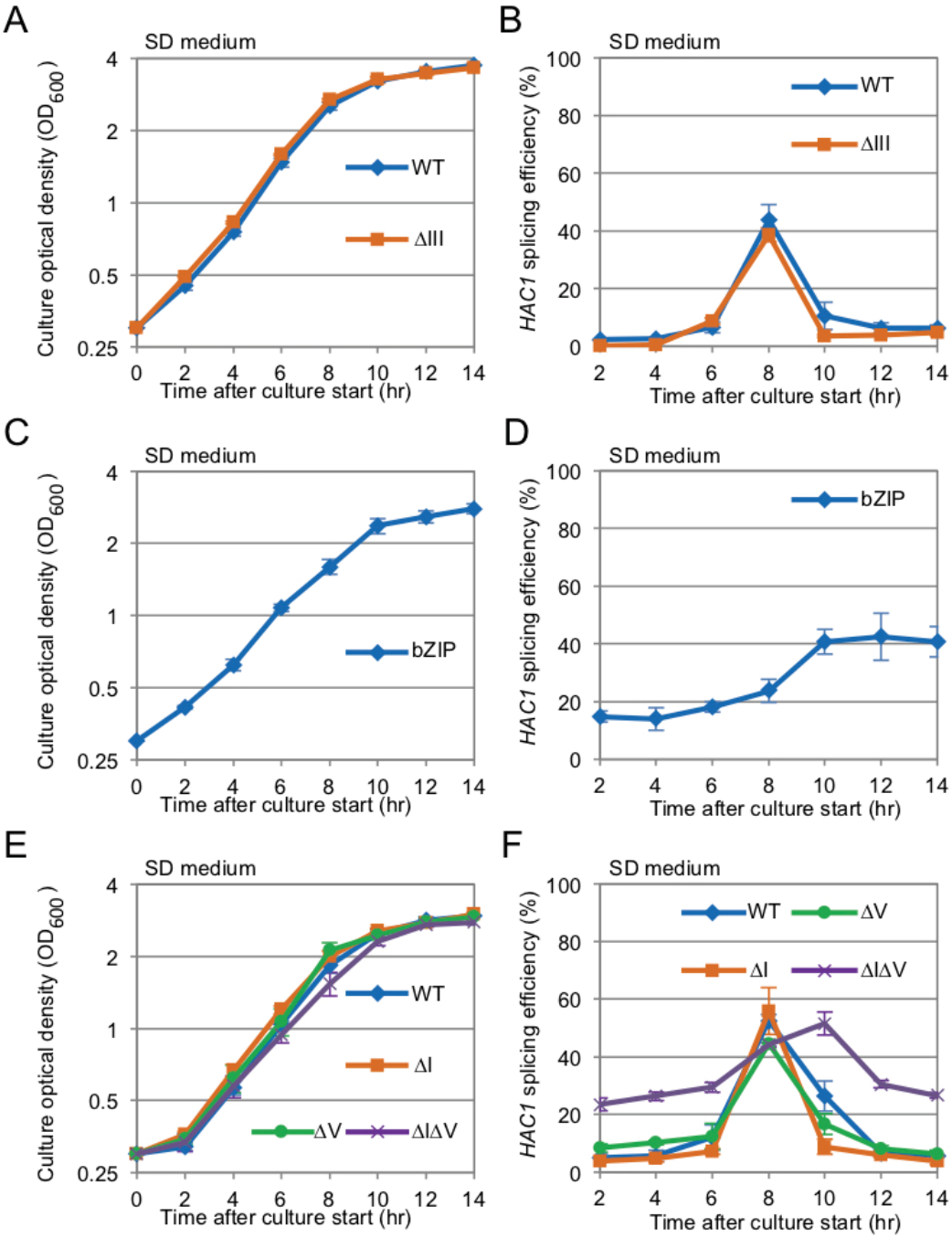


**Figure 12: Effect of the luminal-domain mutations of Ire1 on the *HAC1* mRNA-splicing profile along long-time culturing of yeast cells.** Cells carrying the indicated mutations on the *IRE1* gene were analyzed as done in Figs 7A and C.

### 3.6. ROS is a possible mediator for activation of Ire1 along aerobic respiration of yeast cells.

My findings presented so far strongly suggest a tight relationship between Ire1's activation and the mitochondrial respiration, which is accompanied with ROS production. I then hypothesized that ROS may contributes to induction of the *HAC1*-mRNA splicing caused by diauxic shift. This idea was verified through addition of the ROS scavenger N-acetyl-L-cysteine (NAC) into cultures of *IRE1*+ cells, which slowed cellular growth probably because of an ambiguous cytotoxicity of this chemical (Fig. 13A). Importantly, NAC almost completely abolished the *HAC1*-mRNA splicing upon diauxic shift (Fig. 13B). It also should be noted that conventional ER stressors, DTT and tunicamycin, potently induced the *HAC1*-mRNA splicing both in the presence and absence of NAC (Fig. 13C).

In the experiment shown Fig 13D, exponentially growing *IRE1*+ cells were treated with hydrogen peroxide, which did not induce the *HAC1*-mRNA splicing. However, hydrogen peroxide stimulated the *HAC1*-mRNA splicing in cells carrying the bZIP mutant version of Ire1. I thus assume that the transmembrane or the cytosolic domain of Ire1 is influenced by ROS, which contributes to but is not sufficient for the UPR evocation.

The experiment shown in Figs 14A and B supports our proposal that *HAC1*-mRNA splicing is tightly linked to aerobic respiration and ROS production. Yeast cells are known to be predominantly fueled by aerobic respiration in a non-fermentable glycerol-based medium. When wild-type cells fermentatively growing in SD medium were transferred to SCGlycerol medium, they exhibited a potent ROS production and a considerable and continuing *HAC1*-mRNA splicing (Figs 14B and S1D). Intriguingly, NAC did not inhibit but did support cellular growth after shifting to SCGlycerol (Fig. 14A). We thus think that, under this condition, ROS stress is too severe for cells to grow and to attenuate the Ire1 activation. As expected, NAC abolished the *HAC1*-mRNA splicing under this culturing condition (Fig. 14B).

Meanwhile, when wild-type cells were transferred from SCGlycerol pre-culture to SCGlycerol, the *HAC1*-mRNA splicing was gradually induced (Fig. 14D). This phenomenon is also likely dependent on intracellular ROS, because it was abolished by NAC (Fig. 14E).

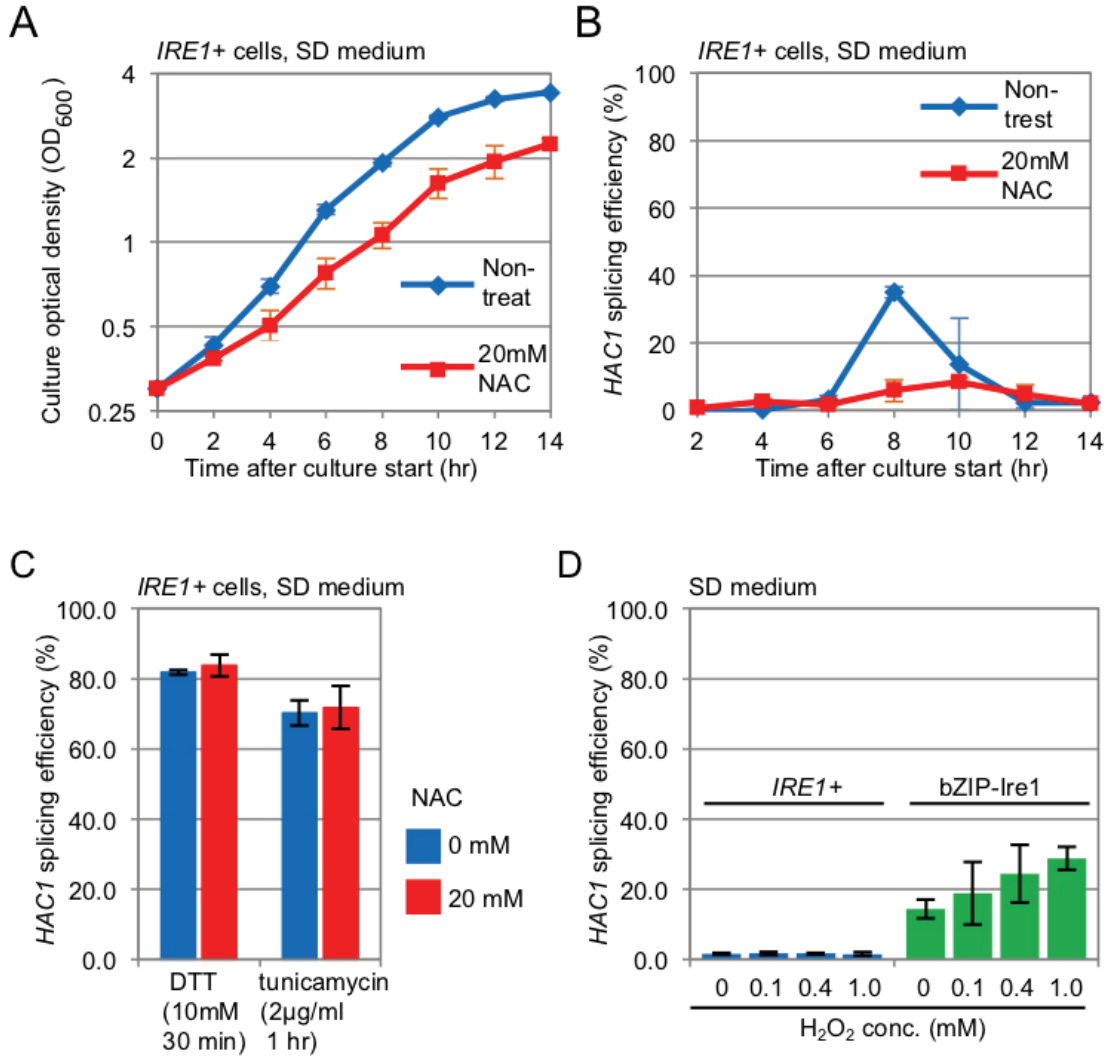


**Figure 13: ROS possibly contributes to but is not sufficient for the Ire1 activation upon diauxic shift.** (A) and (B) *IRE1*+ cells were cultured in the presence or absence of 20 mM NAC and monitored for growth and *HAC1*- mRNA splicing. (C) *IRE1*+ cells were treated with ER-stressing chemicals as indicated and checked for *HAC1*-mRNA splicing. NAC and ER stressors were simultaneously added into cultures. (D) Cells carrying wild-type Ire1 or its b-ZIP mutant version were treated with the indicated concentrations of hydrogen peroxide or remain unstressed, and checked for *HAC1*-mRNA splicing.

Figure 14

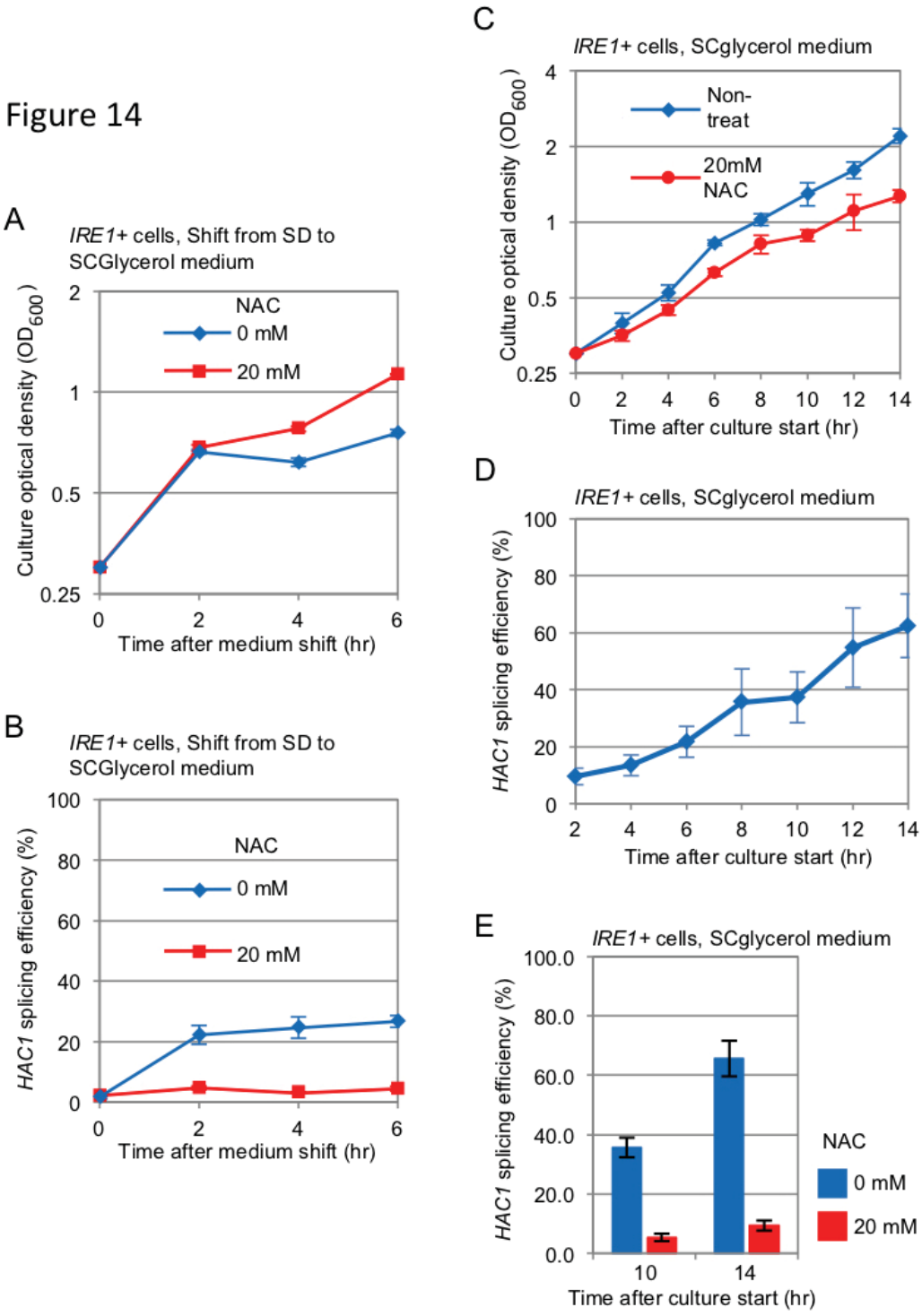


**Figure 14: Induction of the *HAC1*-mRNA splicing in cells cultured in a non- fermentable medium**. (A) and (B) *IRE1*+ cells exponentially growing in SD medium were shifted to SCGlycerol medium at time 0, and further incubated for the indicated durations. (C) to (E) *IRE1*+ cells pre-cultured in SCGlycerol medium were transferred to fresh SCGlycerol medium at time 0, and further incubated for the indicated durations. For "20mM NAC" samples, NAC was added into culture at time 0.

### 3.7. Ire1-dependent expansion of the mitochondria along aerobic respiration of yeast cells.

According to Thibault et al. (2011), the downstream target genes of the UPR in yeast cells vary dependently on the type of stressing stimuli. I thus compared the Ire1-dependent transcriptional change caused by diauxic shift with that caused by canonical ER-stressing stimulus. In the experiments shown in Fig. 15A and Table S1, I performed RNA-sequencing-based transcriptome analysis of *IRE1*+ cells and *ire1Δ* cells stressed by tunicamycin or being on diauxic shift. Fig. 15A indicates a positive correlation between the *IRE1*-dependent transcriptome change in tunicamycin-stressed cells (Y-axis) and that in cells on diauxic shift (X-axis). Indeed, expression of some previously described UPR target genes, for example, *KAR2*, *PDI1* and *TSA1* (Kimata et al., 2006) were induced dependently on Ire1 in response to both canonical ER stressing stimuli (DTT or tunicamycin) and diauxic shift (Figs 15B to D).

Meanwhile, expression of genes carried on the mitochondrial genome upon diauxic shift but not upon tunicamycin stress seemed to be highly dependent on Ire1 (Fig. 15A). Time-course expression monitoring of *OLI1*, which serves as an example of the mitochondrial encoded genes, confirmed that its upregulation along diauxic shift is impaired by the *ire1Δ* mutant (Fig. 15E). Since *hac1Δ* cells exhibited a similar result (Fig. 15F), I think that, as well as in the case of the UPR induced by canonical ER stressors, *HAC1* contributes to *OLI1* expression upon diauxic shift as the proximate target of Ire1.

In the experiments shown in Figs 15G and 16, I compared mitochondria-related cellular statuses between *IRE1*+ cells and *ire1Δ* cells. As the post-diauxic samples, I employed 12-hr cultured cells, since under this condition, cell death was not yet obvious (Fig. 10C). Fig. 15G shows that not only the RNA level but also the DNA level of *OLI1* was induced dependently on Ire1. I thus think that Ire1 increases the mitochondrial RNA abundance, at least partly, through the increment of the mitochondrial DNA abundance. Diauxic shift is known to enlarge mitochondria and to induce respiration, which is accompanied with increment of oxygen uptake. Fig. 16A exhibits cellular level of the mitochondria marker protein Por1, which was induced alongside diauxic shift in *IRE1*+ cells, but poorly in *ire1Δ* cells. According to the data from the transcriptome analysis shown in Table S1, the difference of the cellular Por1 protein level in *IRE1*+ cells and *ire1Δ* cells does not seem to be due to the transcription level of the *POR1* gene. In the experiment shown in Figs 16B and C, mitochondria in *IRE1*+and *ire1Δ* cells in the post-diauxic-shift phase were visualized by mitochondria-located GFP. While mitochondria exhibited tubular-like shape in both types of cells, a quantitative image analysis indicated that mitochondria are less expanded in *ire1Δ* cells. Supporting these insight, oxygen uptake in the post-diauxic-shift phase was lowered by the *ire1Δ* mutation (Fig. 16D).

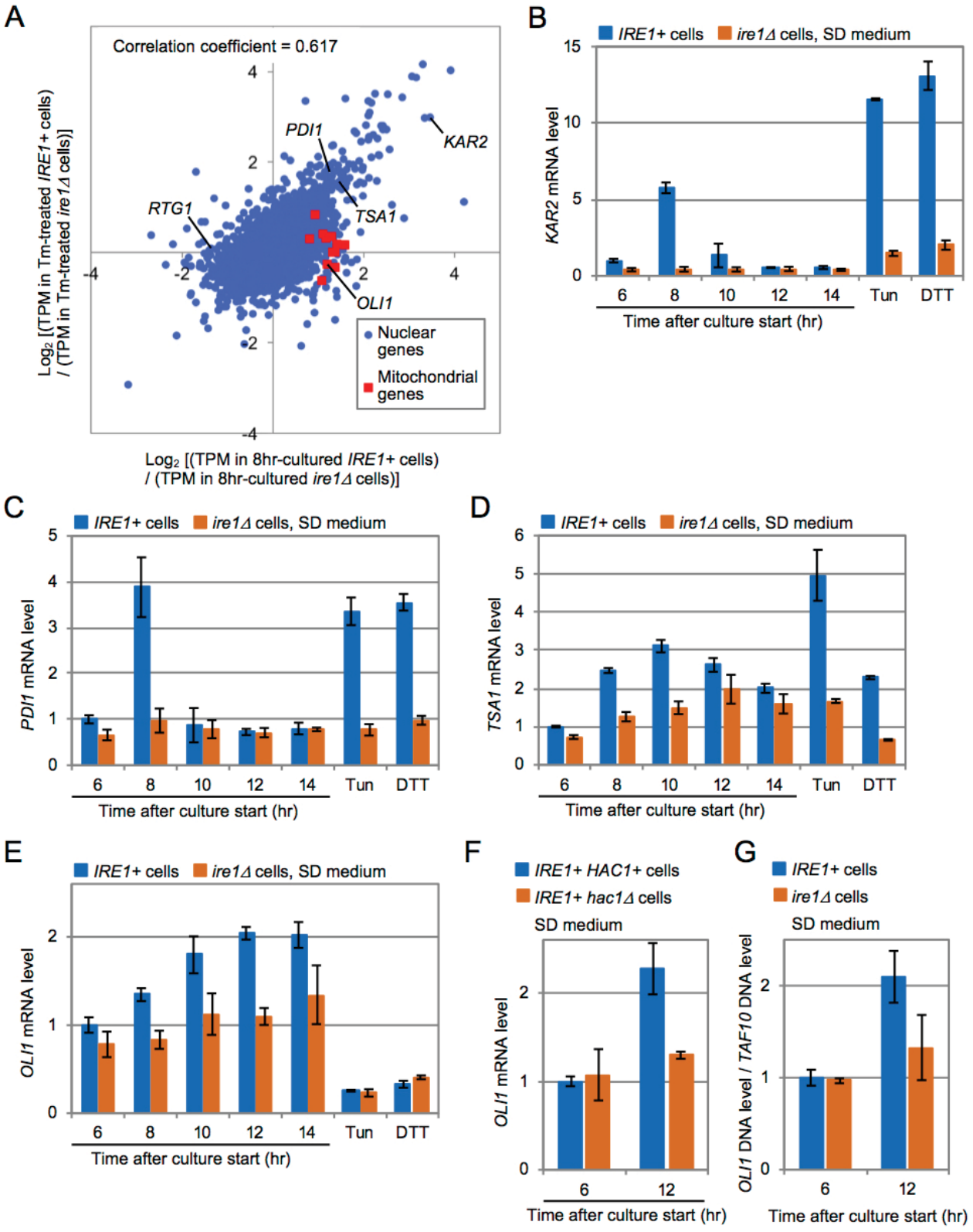
A
Correlation coefficient = 0.617
PDI1
KAR2
RTG1
TSA1
OLI1
Nuclear genes
Mitochondrial genes
Log2 [(TPM in Tm-treated IRE1+ cells) / (TPM in Tm-treated ire1Δ cells)]
Log2 [(TPM in 8hr-cultured IRE1+ cells) / (TPM in 8hr-cultured ire1Δ cells)]
B
IRE1+ cells
ire1Δ cells, SD medium
KAR2 mRNA level
Time after culture start (hr)
Tun
DTT
C
PDI1 mRNA level
D
TSA1 mRNA level
E
OLI1 mRNA level
F
IRE1+ HAC1+ cells
IRE1+ hac1Δ cells
SD medium
G
IRE1+ cells
ire1Δ cells
OLI1 DNA level / TAF10 DNA level

**Figure 15: Ire1-dependent change of gene-expression profile under different conditions.** (A) *IRE1+* cells (two clones) and *ire1Δ* cells (two clones) on diauxic shift (8 hrs-culturing in SD medium) or under canonical ER stress condition (2 μg tunicamycin (Tun) of 1 hr) were subjected to illumina-based RNA sequencing and gene-expression profiling. The resulting TPM (transcripts per million) values of the resulting clones were used to calculate the x-axis and y-axis values of each gene. In this scatter plot, each dot represents one gene (5854 genes in total). Genes with the TPM values of less than 1.00 under any conditions were not plotted. Moreover, the *ULI1* gene is plotted out of the graph area and thus is not shown here. (B) to (E) *IRE1+* cells and *ire1Δ* cells were cultured in SD medium with or without the indicated external stress, and checked for the abundance of mRNAs of the indicated genes using the RT-qPCR technique. (F) The same experiment as done in panel E was performed using *hac1*D cells instead of *ire1Δ* cells. (G) Total DNA samples were analyzed by qPCR using *OLI1*-gene (mitochondria genome) specific and *TAF10*-gene (nuclear genome) specific primers. Expression levels of each gene (or ratios of *OLI1* DNA level to *TAF10* DNA level) are normalized against that of *IRE1+* cells at time 6 hours, which is set at 1.00.

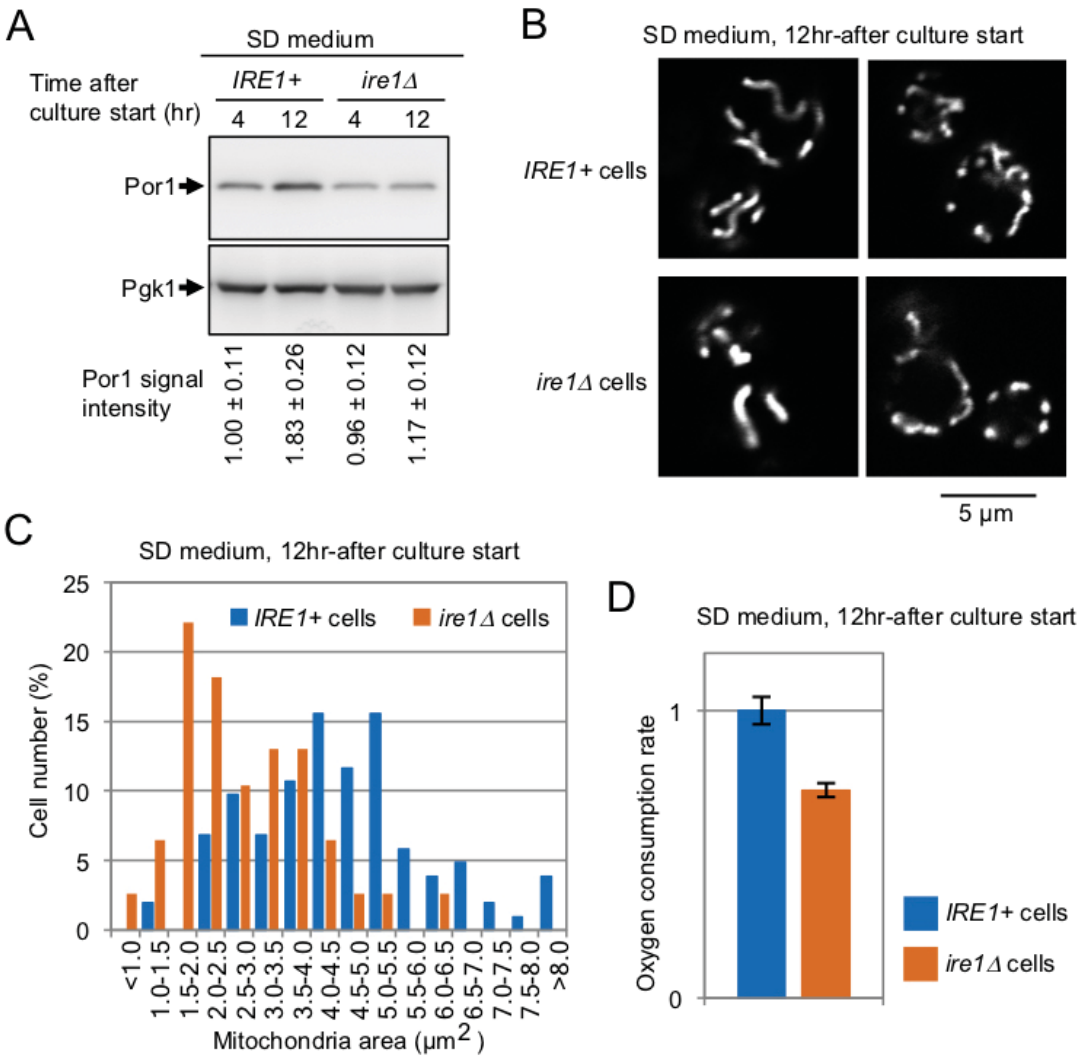


**Figure 16: Ire1-dependent enhancement of respiration and mitochondria size alongside diauxic shift.** *IRE1+* cells and *ire1Δ* cells were cultured in SD medium for the indicated durations. (A) Cell lysates (equivalent to 0.22 OD600 cells) were analyzed by anti-Por1 Western blotting. Anti-Pgk1 Western blot serves as a loading control. (B) and (C) Cells producing mitochondria-located GFP were optically sectioned by a confocal microscope and monitored for fluorescing area. (D) Oxygen consumption rates were assayed as described in the Materials and Methods section.

# CHAPTER IV
# DISCUSSION

As its name denotes, the UPR has been believed to be a cellular response against accumulation of unfolded proteins in the ER lumen. Indeed, it is highly likely that the luminal domain of Ire1 has an ability to directly capture unfolded proteins, which leads to activation of Ire1 and evocation of the UPR (Credle et al., 2005; Kimata et al., 2007; Promlek et al., 2011; Gardner et al., 2011; Karagoz et al., 2017). Meanwhile, in the present study, I cultured yeast cells in two media, YPD and SD, which are the most commonly used media in laboratories, for long duration and noticed that the UPR is transiently induced upon diauxic shift (Figs 7, S2 and S3). Intriguingly, this phenomenon is unlikely to accompany ER accumulation of unfolded proteins, since, in this case, wild-type Ire1 and the ΔIII mutant of Ire1 were equally activated (Figs 12A and B). Moreover, the protein-folding status in the ER does not seems to be harmed upon diauxic shift (Fig 11).

The transient induction of the UPR was poorly observed in $\rho^0$ cells or in wild-type cells cultured with antimycin A (Fig. 9), and thus appears to be tightly linked to mitochondrial respiration. Consistently with this idea, the UPR was highly and quickly induced when cells were shifted to non-fermentable glycerol-based medium (Fig. 14B). This observation argues against an idea that activation of Ire1 shown in Fig. 1 may be caused by exhaustion of trace nutrient components from medium along long-time culturing. Because NAC considerably impaired the UPR induction along aerobic respiration (Figs 13A, 13B and 14), ROS probably serve as mediators for the UPR induction in this case. By considering the susceptibility of bZIP-Ire1 to hydrogen peroxide (Fig. 13D), I assume that ROS contributes to activation of Ire1 through directly or indirectly acting to its cytosolic or transmembrane domain. In contrast, unlike in the case of bZIP-Ire1 cells, hydrogen peroxide did not induce the UPR in *IRE1*+ cells carrying wild-type Ire1 (Fig. 13D). Moreover, the UPR upon diauxic shift was transient in *IRE1*+ cells (Fig. 7), while cellular level of ROS remained high even after diauxic shift (Fig. S1A). This observation supports my idea that ROS is not sufficient for the UPR induction. It should be also noted that bZIP Ire1 was continuingly activated after diauxic shift (Figs 12C and D).

These observations can be explained by the fact that bZIP-Ire1 is an easy-to-activate mutant which bypasses regulation on the luminal region. It is likely that bZIP-Ire1 is hypersensitive to ROS. As a possible and hypothetical explanation for the ROS hypersensitivity of bZIP-Ire1, we propose a hypothetical scenario which is illustrated in Fig. 17. Diauxic shift influences to Ire1 via two different ways to Ire1, both of which is required for activation of

Ire1. One is ROS, which directly or indirectly works on the cytosolic domain (or the transmembrane domain) of Ire1. The other signal is still obscure and works on the luminal domain of Ire1. Because of the absence of the latter signal, wild-type Ire1 is not activated by ROS only. Moreover, because the latter signal is quickly attenuated, activation of wild-type Ire1 upon diauxic shift is only transient.

My laboratory previously reported that Subregion V serves as the BiP-binding site, which negatively regulates Ire1 (Kimata et al., 2004). Moreover, Subregion I is likely to be intramolecularly associated with the cLD of Ire1 and inhibits its self-association under non-stress conditions (Mathuranyanon et al., 2015). According to my observation shown in Figs 12E and F, as well as *IRE1*+ cells, cells carrying the ΔIΔV version of Ire1 evoked the UPR transiently upon diauxic shift. I thus speculate that neither Subregion I nor V plays an important role for the transient UPR induction observed in this study.

Here I also show that the Ire1-dependent *HAC1* splicing upon diauxic shift contributes to growth and survival of yeast cells (Fig. 10). As well as in the case of canonical ER stressing stimuli, Ire1 controls expression of a number of genes (Fig. 15A), which includes the peroxiredoxin gene Tsa1 (Fig. 15D). Thus one of the physiological meaning of the UPR induction upon diauxic shift may be to cope with ROS, which is byproducts of respiration. Meanwhile, I also found Ire1-dependent increment of the mRNA level of mitochondrial genes upon diauxic shift (Figs 15A and E). This phenomenon does not seem to be solely due to transcriptional induction of the mitochondrial genes, since the cellular level of the mitochondrial DNA was also increased under this condition (Fig. 15G). My observations shown in Fig. 16 indicate Ire1-dependent enhancement of size and function of the mitochondria alongside diauxic shift. However, canonical ER-stressing stimuli repressed the *OLI1* expression level independently of Ire1. This observation argues that an outcome of the Ire1 activation upon diauxic shift differs from that caused by canonical ER-stressing stimuli, implying complexity of intercellular signaling pathways that interact with the Ire1/HAC1-dependent UPR signaling pathway.

As a possible molecular basis underlying dependency of mitochondria expansion on the Ire1-*HAC1* pathway, the UPR induces a wide variety of genes including those encoding enzymes for membrane-lipid biogenesis (Travers et al., 2000; Kimata et al., 2006), which should be required for mitochondria expansion. The contribution of ER-to-mitochondria lipid transport to maintenance of mitochondria homeostasis and integrity is reviewed in Scharwey et al. (2013). Moreover, Isc1, a sphingolipid biosynthetic-pathway enzyme, is reported to be required for enhancement of mitochondrial functions upon diauxic shift (Kitagaki et al., 2009).

On the other hand, I do not think that induction of the mitochondrial DNA replication is a direct downstream phenomenon upregulated by the Ire1-HAC1 pathway upon diauxic shift. This is because, according to the RNA-sequencing analysis shown in 15A, expression of genes related to mitochondrial DNA replication is not under control of Ire1. Rather, I assume that the low abundance of the mitochondrial DNA in *ire1Δ* cells on post-diauxic-shift phase (Fig. 15G) is a result (but not the cause) of the impairment of mitochondrial expansion shown in Fig 16.

It should be noted that Ire1 is activated upon diauxic shift only transiently, while phenotypes of *ire1Δ* cells (*e.g.* slow growth, low respiration, and less expanded mitochondria) were observable even on the post-diauxic-shift phase. We think that the mitochondrial expansion is a phenomenon that occurs upon diauxic shift along the Ire1 activation, contributing to aerobic respiration and cellular growth during the post-diauxic-shift phase. In other words, the transient activation of Ire1 upon diauxic shift is a preparation for the next stage, aerobic respiration. Meanwhile, it may be also possible that faint activity of Ire1 on the post-diauxic-shift phase is somehow conductive to aerobic respiration and cellular growth on that time point.

In conclusion, here I describe induction of the Ire1-*HAC1* pathway of the UPR along mitochondrial aerobic respiration in yeast cells (Fig. 17). For this phenomenon, ROS serve as possible mediators, which appear to act to the cytosolic domain of Ire1, while they are not sufficient for activation of Ire1. Evocation of the UPR under this condition leads to expansion of the mitochondria and to stimulation of respiration, as well as the canonical transcriptome change upon ER stress. Since respiration generates ROS as byproducts, the UPR induction alongside diauxic shift can be considered as a positive feedback regulation. Taken together, I propose here a new mode of action of the Ire1-*HAC1* signaling pathway of the UPR, which argues for a novel aspect of intracellular communication of two different organelles, the ER and the mitochondria, in yeast cells.

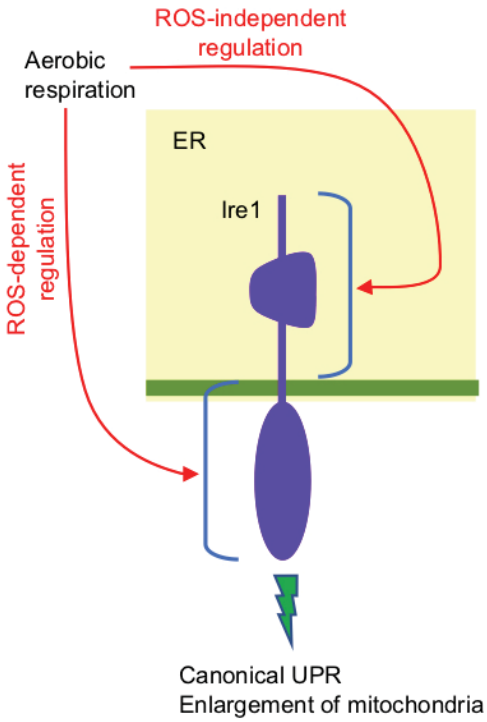


**Figure 17: Activation of Ire1 along aerobic respiration in yeast cells.** Novel activation mode and role of Ire1 presented in this study is illustrated.

**ACKNOWLEDGEMENT**

From bottom of my heart, I would like to express my sincere gratitude to my supervisor Assoc. Prof. Yukio Kimata for his enthusiastic guidance, helpful suggestion, kindly support and especially, his patience. He was not only my supervisor but also my teacher, he taught me everything from how to think as a scientist to how to solve problems when it occurs during study. I really appreciate him for that.

Also, I would like to thank my advisors, Prof. Hisaji Maki and Prof. Kaz Shiozaki for their constructive comments and valuable advises on my research.

I am extremely grateful to Prof. Kenji Kohno and Prof. Hiroshi Takagi for their helpful discussion and allowing me to conduct my study in their laboratory.

I would like to thank Dr. Yuki Ishiwata-Kimata for her helpful advises and positive discussion.

I also would like to thank all of members in Molecular and Cell Genetics Laboratory and Applied Stress Microbiology Laboratory for their help during my PhD course.

I gratefully acknowledge financial support from NAIST Global COE that made my PhD work possible.

I would not be successful without supports from my family and my friends. Thanks to them who always stand by me and encourage me moving forward whenever I have had troubles with my study. Finally, I want to express my special thanks to my wife for her support and for taking care of my daughter during my stay in Japan.

Tran Minh Duc

## REFERENCES

Aragon, T., van Anken, E., Pincus, D., Serafimova, I. M., Korennykh, A. V., Rubio, C. A., and Walter, P. (2009) Messenger RNA targeting to endoplasmic reticulum stress signalling sites. *Nature* 457: 736-740.

Bertolotti, A., Zhang, Y., Hendershot, L. M., Harding, H. P., and Ron, D. (2000) Dynamic interaction of BiP and ER stress transducers in the unfolded-protein response. *Nat. Cell Biol.* 2: 326-332.

Carrara, M., Prischi, F., Nowak, P. R., Kopp, M. C., and Ali, M. M. (2015) Noncanonical binding of BiP ATPase domain to Ire1 and Perk is dissociated by unfolded protein CH1 to initiate ER stress signaling. *eLife* 4: e03522.

Casagrande, R., Stern, P., Diehn, M., Shamu, C., Osario, M., Zuniga, M., Brown, P. O., and Ploegh, H. (2000) Degradation of proteins from the ER of *S. cerevisiae* requires an intact unfolded protein response pathway. *Mol. Cell* 5: 729-735.

Chawla, A., Chakrabarti, S., Ghosh, G., and Niwa, M. (2011) Attenuation of yeast UPR is essential for survival and is mediated by IRE1 kinase. *J. Cell Biol.* 193: 41-50.

Cox, J. S., Chapman, R. E., and Walter, P. (1997) The unfolded protein response coordinates the production of endoplasmic reticulum protein and endoplasmic reticulum membrane. *Mol. Biol. Cell* 8: 1805-1814.

Cox, J. S., Shamu, C. E., and Walter, P. (1993) Transcriptional induction of genes encoding endoplasmic reticulum resident proteins requires a transmembrane protein kinase. *Cell* 73: 1197-1206.

Cox, J. S., and Walter, P. (1996) A novel mechanism for regulating activity of a transcription factor that controls the unfolded protein response. *Cell* 87: 391-404.

Credle, J. J., Finer-Moore, J. S., Papa, F. R., Stroud, R. M., and Walter, P. (2005) On the mechanism of sensing unfolded protein in the endoplasmic reticulum. *Proc. Natl. Acad. Sci. USA* 102: 18773-18784.

DeRisi, J. L., Iyer, V. R., and Brown, P. O. (1997) Exploring the metabolic and genetic control of gene expression on a genomic scale. *Science* 278: 680-686.

Di Santo, R., Aboulhouda, S., and Weinberg, D. E. (2016) The fail-safe mechanism of post-transcriptional silencing of unspliced *HAC1* mRNA. *eLife* 5: e20069.

Egner A, Jakobs S, Hell SW. (2002). Fast 100-nm resolution three dimensional microscope reveals structural plasticity of mitochondria in live yeast. *Proc. Natl. Acad. Sci. USA* 99: 3370-5

Fordyce, P. M., Pincus, D., Kimmig, P., Nelson, C. S., El-Samad, H., Walter, P., and DeRisi, J. L. (2012) Basic leucine zipper transcription factor Hac1 binds DNA in two distinct modes as revealed by microfluidic analyses. *Proc. Natl. Acad. Sci. USA* 109: E3084-E3093.

Friedlander, R., Jarosch, E., Urban, J., Volkwein, C., and Sommer, T. (2000) A regulatory link between ER-associated protein degradation and the unfolded-protein response. *Nat. Cell Biol.* 2: 379-384.

Gardner, B. M., and Walter, P. (2011) Unfolded proteins are Ire1-activating ligands that directly induce the unfolded protein response. *Science* 333: 1891-1894.

Gonzalez, T. N., Sidrauski, C., Dorfler, S., and Walter, P. (1999) Mechanism of non-spliceosomal mRNA splicing in the unfolded protein response pathway. *EMBO J.* 18: 3119-3132.

Halbleib, K., Pesek, K., Covino, R., Hofbauer, H. F., Wunnicke, D., Hanelt, I., Hummer, G., and Ernst, R. (2017) Activation of the unfolded protein response by lipid bilayer stress. *Mol. Cell* 67: 673-684 e678.

Hiller, M. M., Finger, A., Schweiger, M., and Wolf, D. H. (1996) ER degradation of a misfolded luminal protein by the cytosolic ubiquitin-proteasome pathway. *Science* 273: 1725-1728.

[a]Ishiwata-Kimata, Y., Yamamoto, Y. H., Takizawa, K., Kohno, K., and Kimata, Y. (2013) F-actin and a type-II myosin are required for efficient clustering of the ER stress sensor Ire1. *Cell Struct. Funct.* 38: 135-143.

[b]Ishiwata-Kimata, Y., Promlek, T., Kohno, K., and Kimata, Y. (2013) BiP-bound and nonclustered mode of Ire1 evokes a weak but sustained unfolded protein response. *Genes Cells* 18: 288-301.

Karagoz, G. E., Acosta-Alvear, D., Nguyen, H. T., Lee, C. P., Chu, F., and Walter, P. (2017) An unfolded protein-induced conformational switch activates mammalian IRE1. *eLlife* 6.

Kawahara, T., Yanagi, H., Yura, T., and Mori, K. (1998) Unconventional splicing of HAC1/ERN4 mRNA required for the unfolded protein response. Sequence-specific and non-sequential cleavage of the splice sites. *J. Biol. Chem.* 273: 1802-1807.

Kawazoe, N., Kimata, Y., and Izawa, S. (2017) Acetic acid causes endoplasmic reticulum stress and induces the unfolded protein response in *Saccharomyces cerevisiae*. *Front Microbiol.* 8: 1192.

Kimata, Y., Ishiwata-Kimata, Y., Ito, T., Hirata, A., Suzuki, T., Oikawa, D., Takeuchi, M., and Kohno, K. (2007) Two regulatory steps of ER-stress sensor Ire1 involving its cluster formation and interaction with unfolded proteins. *J. Cell Biol.* 179: 75-86.

Kimata, Y., Ishiwata-Kimata, Y., Yamada, S., and Kohno, K. (2006) Yeast unfolded protein response pathway regulates expression of genes for anti-oxidative stress and for cell surface proteins. *Genes Cells* 11: 59-69.

Kimata, Y., Kimata, Y. I., Shimizu, Y., Abe, H., Farcasanu, I. C., Takeuchi, M., Rose, M. D., and Kohno, K. (2003) Genetic evidence for a role of BiP/Kar2 that regulates Ire1 in response to accumulation of unfolded proteins. *Mol. Biol. Cell* 14: 2559-2569.

Kimata, Y., and Kohno, K. (2011) Endoplasmic reticulum stress-sensing mechanisms in yeast and mammalian cells. *Curr. Opin. Cell Biol.* 23: 135-142.

Kimata, Y., Oikawa, D., Shimizu, Y., Ishiwata-Kimata, Y., and Kohno, K. (2004) A role for BiP as an adjustor for the endoplasmic reticulum stress-sensing protein Ire1. *J. Cell Biol*. 167: 445-456.

Kitagaki, H., Cowart, L. A., Matmati, N., Montefusco, D., Gandy, J., de Avalos, S. V., Novgorodov, S. A., Zheng, J., Obeid, L. M., and Hannun, Y. A. (2009) ISC1-dependent metabolic adaptation reveals an indispensable role for mitochondria in induction of nuclear genes during the diauxic shift in Saccharomyces cerevisiae. *J. Biol. Chem*. 284: 10818-10830.

Kohno, K., Normington, K., Sambrook, J., Gething, M. J., and Mori, K. (1993) The promoter region of the yeast KAR2 (BiP) gene contains a regulatory domain that responds to the presence of unfolded proteins in the endoplasmic reticulum. *Mol. Cell. Biol*. 13: 877-890.

Korennykh, A. V., Egea, P. F., Korostelev, A. A., Finer-Moore, J., Zhang, C., Shokat, K. M., Stroud, R. M., and Walter, P. (2009) The unfolded protein response signals through high-order assembly of Ire1. *Nature* 457: 687-693.

Kozutsumi, Y., Segal, M., Normington, K., Gething, M. J., and Sambrook, J. (1988) The presence of malfolded proteins in the endoplasmic reticulum signals the induction of glucose-regulated proteins. *Nature* 332: 462-464.

Le, Q. G., Ishiwata-Kimata, Y., Kohno, K., and Kimata, Y. (2016) Cadmium impairs protein folding in the endoplasmic reticulum and induces the unfolded protein response. *FEMS Yeast Res*. 16: fow049.

Lee, K. P., Dey, M., Neculai, D., Cao, C., Dever, T. E., and Sicheri, F. (2008) Structure of the dual enzyme Ire1 reveals the basis for catalysis and regulation in nonconventional RNA splicing. *Cell* 132: 89-100.

Mathuranyanon, R., Tsukamoto, T., Takeuchi, A., Ishiwata-Kimata, Y., Tsuchiya, Y., Kohno, K., and Kimata, Y. (2015) Tight regulation of the unfolded protein sensor Ire1 by its intramolecularly antagonizing subdomain. *J. Cell Sci*. 128: 1762-1772.

Mai, C. T., Le Q. G., Ishiwata-Kimata Y., Takagi H., Kohno K., and Kimata Y. (2018) 4-Phenylbutyrate suppresses the unfolded protein response without restoring protein folding in Saccharomyces cerevisiae. *FEMS Yeast Res*. 18: foy016.

Merksamer, P. I., Trusina, A., and Papa, F. R. (2008) Real-time redox measurements during endoplasmic reticulum stress reveal interlinked protein folding functions. *Cell* 135: 933-947.

Miyagawa, K., Ishiwata-Kimata, Y., Kohno, K., and Kimata, Y. (2014) Ethanol stress impairs protein folding in the endoplasmic reticulum and activates Ire1 in *Saccharomyces cerevisiae*. *Biosci. Biotechnol. Biochem*. 78: 1389-1391.

Mori, K., Kawahara, T., Yoshida, H., Yanagi, H., and Yura, T. (1996) Signalling from endoplasmic reticulum to nucleus: transcription factor with a basic-leucine zipper motif is required for the unfolded protein-response pathway. *Genes Cells* 1: 803-817.

Mori, K., Ma, W., Gething, M. J., and Sambrook, J. (1993) A transmembrane protein with a cdc2+/CDC28-related kinase activity is required for signaling from the ER to the nucleus. *Cell* 74: 743-756.

Mori, K., Ogawa, N., Kawahara, T., Yanagi, H., and Yura, T. (2000) mRNA splicing-mediated C-terminal replacement of transcription factor Hac1p is required for efficient activation of the unfolded protein response. *Proc. Natl. Acad. Sci. USA* 97: 4660-4665.

Mori, K., Sant, A., Kohno, K., Normington, K., Gething, M. J., and Sambrook, J. F. (1992) A 22 bp cis-acting element is necessary and sufficient for the induction of the yeast KAR2 (BiP) gene by unfolded proteins. *EMBO J*. 11: 2583-2593.

Nguyen, T. S., Kohno, K., and Kimata, Y. (2013) Zinc depletion activates the endoplasmic reticulum-stress sensor Ire1 via pleiotropic mechanisms. *Biosci. Biotechnol. Biochem*. 77: 1337-1339.

Nikawa, J., Sugiyama, M., Hayashi, K., and Nakashima, A. (1997) Suppression of the *Saccharomyces cerevisiae* hac1/ire15 mutation by yeast genes and human cDNAs. *Gene* 201: 5-10.

Niwa, M., Patil, C. K., DeRisi, J., and Walter, P. (2005) Genome-scale approaches for discovering novel nonconventional splicing substrates of the Ire1 nuclease. *Genome Biol*. 6: R3.

Normington, K., Kohno, K., Kozutsumi, Y., Gething, M. J., and Sambrook, J. (1989) *S. cerevisiae* encodes an essential protein homologous in sequence and function to mammalian BiP. *Cell* 57: 1223-1236.

Ohlmeier S, Kastaniotis AJ, Hiltunen JK, Bergmann U. (2004) The Yeast Mitochondrial Proteome, a Study of Fermentative and Respiratory Growth. J Bio Chem. 279: 3956-79

Oikawa, D., Kimata, Y., and Kohno, K. (2007) Self-association and BiP dissociation are not sufficient for activation of the ER stress sensor Ire1. *J. Cell Sci*. 120: 1681-1688.

Oikawa, D., Kimata, Y., Takeuchi, M., and Kohno, K. (2005) An essential dimer-forming subregion of the endoplasmic reticulum stress sensor Ire1. *Biochem. J*. 391: 135-142.

Okamura, K., Kimata, Y., Higashio, H., Tsuru, A., and Kohno, K. (2000) Dissociation of Kar2p/BiP from an ER sensory molecule, Ire1p, triggers the unfolded protein response in yeast. *Biochem. Biophys. Res. Commun*. 279: 445-450.

Papa, F. R., Zhang, C., Shokat, K., and Walter, P. (2003) Bypassing a kinase activity with an ATP-competitive drug. *Science* 302: 1533-1537.

Pincus, D., Chevalier, M. W., Aragon, T., van Anken, E., Vidal, S. E., El-Samad, H., and Walter, P. (2010) BiP binding to the ER-stress sensor Ire1 tunes the homeostatic behavior of the unfolded protein response. *PLoS Biol*. 8: e1000415.

Promlek, T., Ishiwata-Kimata, Y., Shido, M., Sakuramoto, M., Kohno, K., and Kimata, Y. (2011) Membrane aberrancy and unfolded proteins activate the endoplasmic reticulum stress sensor Ire1 in different ways. *Mol. Biol. Cell* 22: 3520-3532.

Rose, M. D., Misra, L. M., and Vogel, J. P. (1989) KAR2, a karyogamy gene, is the yeast homolog of the mammalian BiP/GRP78 gene. *Cell* 57: 1211-1221.

Rubio, C., Pincus, D., Korennykh, A., Schuck, S., El-Samad, H., and Walter, P. (2011) Homeostatic adaptation to endoplasmic reticulum stress depends on Ire1 kinase activity. *J. Cell Biol*. 193: 171-184.

Ruegsegger, U., Leber, J. H., and Walter, P. (2001) Block of *HAC1* mRNA translation by long-range base pairing is released by cytoplasmic splicing upon induction of the unfolded protein response. *Cell* 107: 103-114.

Scharwey, M., Tatsuta, T., and Langer, T. (2013) Mitochondrial lipid transport at a glance. *J. Cell Sci*. 126: 5317-5323.

Shamu, C. E., and Walter, P. (1996) Oligomerization and phosphorylation of the Ire1p kinase during intracellular signaling from the endoplasmic reticulum to the nucleus. *EMBO J*. 15: 3028-3039.

Sidrauski, C., Cox, J. S., and Walter, P. (1996) tRNA ligase is required for regulated mRNA splicing in the unfolded protein response. *Cell* 87: 405-413.

Sidrauski, C., and Walter, P. (1997) The transmembrane kinase Ire1p is a site-specific endonuclease that initiates mRNA splicing in the unfolded protein response. *Cell* 90: 1031-1039.

Sikorski, R. S., and Hieter, P. (1989) A system of shuttle vectors and yeast host strains designed for efficient manipulation of DNA in Saccharomyces cerevisiae. *Genetics* 122: 19-27.

Thibault, G., Ismail, N., and Ng, D. T. (2011) The unfolded protein response supports cellular robustness as a broad-spectrum compensatory pathway. *Proc. Natl. Acad. Sci. USA* 108: 20597-22602.

Travers, K. J., Patil, C. K., Wodicka, L., Lockhart, D. J., Weissman, J. S., and Walter, P. (2000) Functional and genomic analyses reveal an essential coordination between the unfolded protein response and ER-associated degradation. *Cell* 101: 249-258.

Van Anken, E., Pincus, D., Coyle, S., Aragon, T., Osman, C., Lari, F., Gomez Puerta, S., Korennykh, A. V., and Walter, P. (2014) Specificity in endoplasmic reticulum-stress signaling in yeast entails a step-wise engagement of *HAC1* mRNA to clusters of the stress sensor Ire1. *eLife* 3: e05031.

Volmer, R., van der Ploeg, K., and Ron, D. (2013) Membrane lipid saturation activates endoplasmic reticulum unfolded protein response transducers through their transmembrane domains. *Proc. Natl. Acad. Sci. USA* 110: 4628-4633.

Westermann B., and Neupert W. (2000) Mitochondria-targeted green fluorescent proteins: convenient tools for the study of organelle biogenesis in Saccharomyces cerevisiae. *Yeast* 16: 1421-1427.

# SUPPLEMENTAL DATA

**Table S1: Gene expression profile of *IRE1+* cells and *ire1Δ* cells.** The raw TPM data for Fig. 6A are presented. Table S1 is available in the following WEB site.
https://www.dropbox.com/sh/8p8rxy82jrlqfmp/AADNiBtGBOpsTbckMEqu-w4xa?dl=0

Figure S1

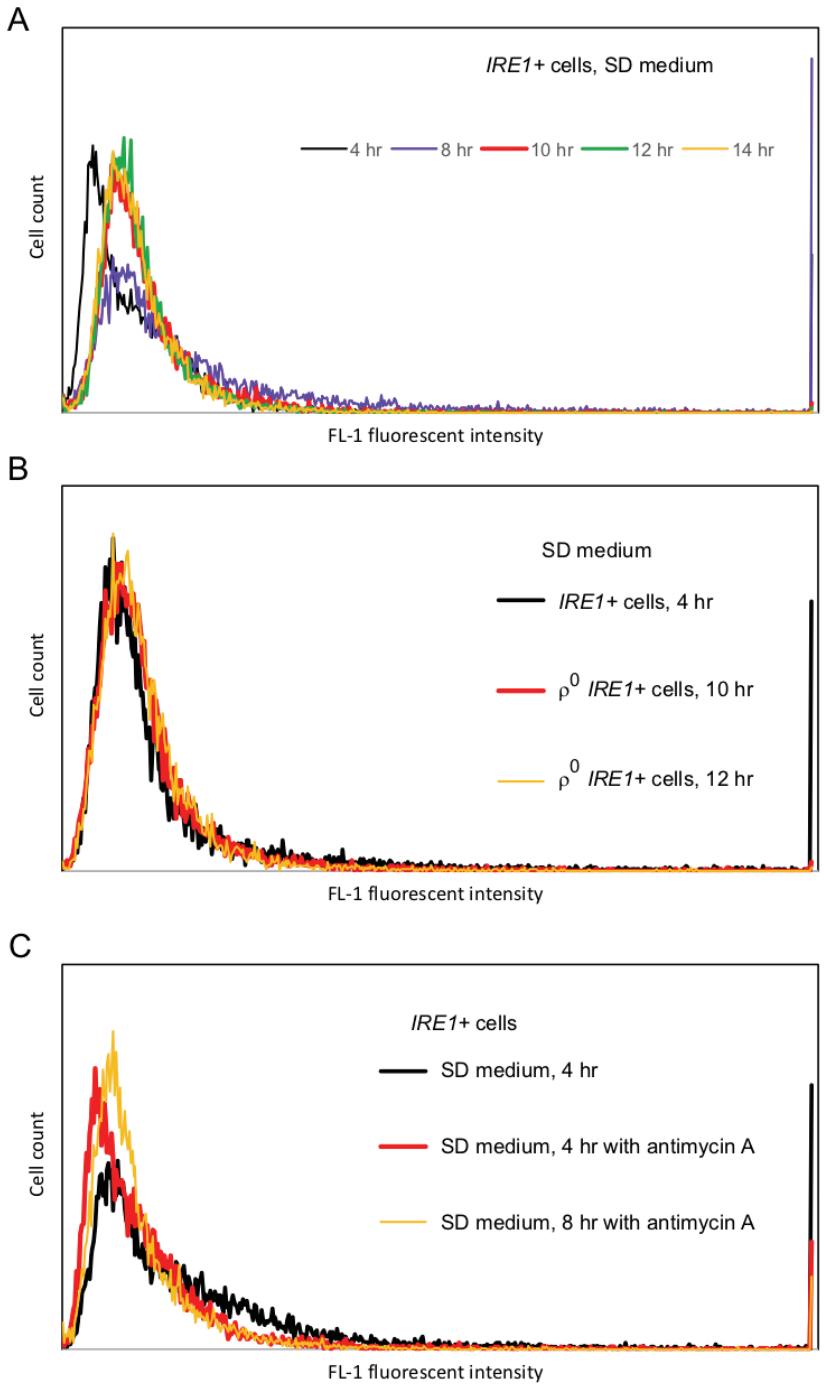

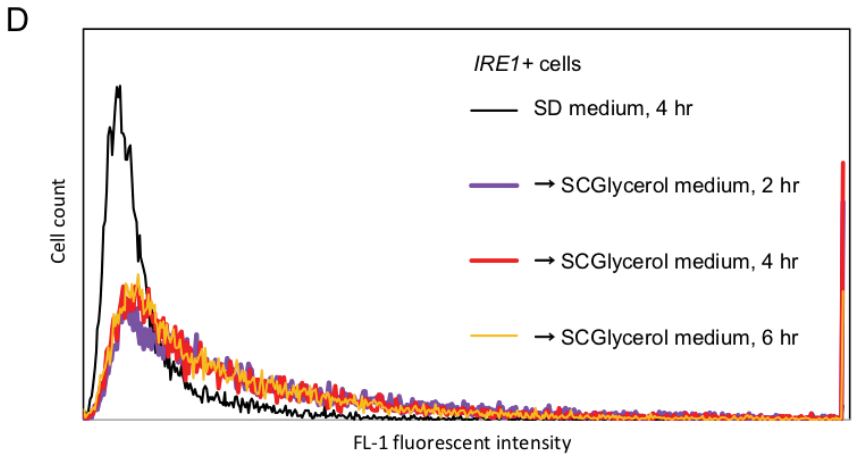


**Figure S1: Accumulation of ROS in yeast cells upon aerobic respiration.**
After being cultured in SD medium (A, B and C) or shifted from SD to SCGlycerol medium (D) for the indicated durations, *IRE1*+ cells or r0 *IRE1*+ cells were stained with DCDHF-DA, which serves as a ROS indicator, and analyzed on an Accuri C6 flow cytometer (BD Biosciences). In panel C, antimycin (2 μg/ml) was added into medium just after culture start.

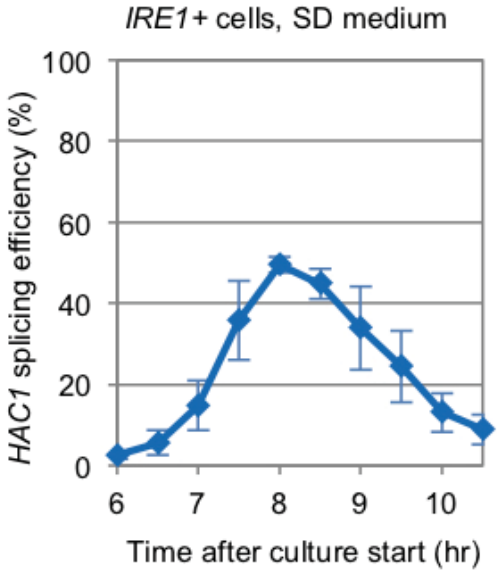


**Figure S2: Detailed time-course profiling of the transient *HAC1* mRNA splicing upon diauxic shift.** The same experiment as done in Fig. 7B was performed with 30-min sampling intervals.

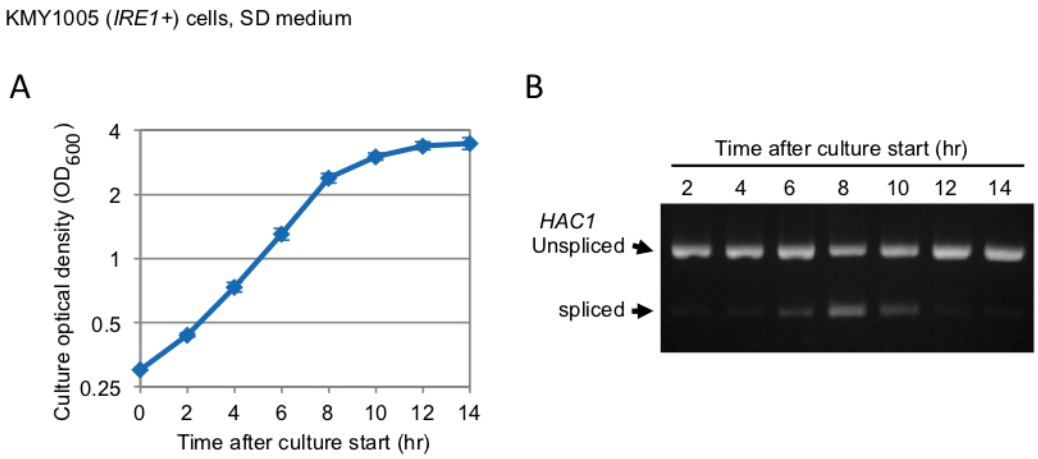


**Figure S3: Transient induction of the *HAC1*-mRNA splicing upon diauxic shift in yeast KMY1005 strain.** KMY1005 cells were cultured in SD medium and checked for cellular growth (A) and the *HAC1*-mRNA splicing (B).

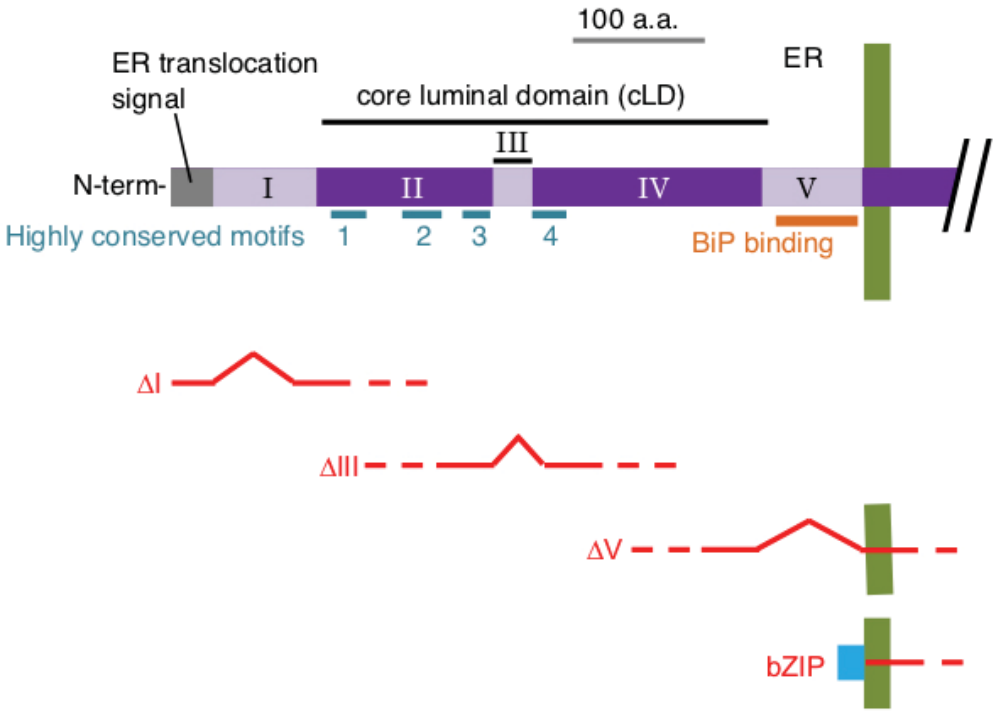


**Figure S4: Structure of the luminal domain of yeast Ire1 and its mutants.**
Segmentation of the luminal domain of yeast Ire1 into Subregions I to V is described in Kimata et al. (2004). The DI, and DIII and DV mutations are deletions of a.a 32-91, a.a. 253-272 and a.a. 463-524 of yeast Ire1, respectively.